

# Clustering-aware Graph Construction: A Joint Learning Perspective

Yuheng Jia, Hui Liu, Junhui Hou, *Member, IEEE*, and Sam Kwong, *Fellow, IEEE*

**Abstract**—Graph-based clustering methods have demonstrated the effectiveness in various applications. Generally, existing graph-based clustering methods first construct a graph to represent the input data and then partition it to generate the clustering result. However, such a stepwise manner may make the constructed graph not fit the requirements for the subsequent decomposition, leading to compromised clustering accuracy. To this end, we propose a joint learning framework, which is able to learn the graph and the clustering result simultaneously, such that the resulting graph is tailored to the clustering task. The proposed method is formulated as a well-defined nonnegative and off-diagonal constrained optimization problem, which is further efficiently solved with convergence theoretically guaranteed. The advantage of the proposed model is demonstrated by comparing with 19 state-of-the-art clustering methods on 10 datasets with 4 clustering metrics.

**Index Terms**—Adaptive graph learning, Clustering.

## I. INTRODUCTION

Clustering aims to partition the input data into different groups, where the samples in the same group are more similar to each other than to those in other groups. Many real-world applications can be formulated as a clustering problem, e.g., image segmentation [1], [2], image classification [3], community detection [4], recommender system [5], tumor discovery [6], [7], [8], and data visualization [9]. Over the past several decades, many clustering methods were proposed like K-means, Gaussian mixture models (GMM) [10], mean shift [11], [12], and various graph-based clustering methods [13], [14], [15], [16], [17]. Particularly, graph-based clustering methods have achieved impressive performance in various applications, which represent input data with a graph, and then partition the graph into subgraphs. The representative graph-based clustering methods are spectral clustering (SC) [13], [14], [17] and symmetric nonnegative matrix factorization (SymNMF) [15], [16].

How to build a reasonable graph plays a critical role in graph-based clustering, since the quality of the graph usually determines the final clustering performance seriously. The most-well known graph construction method is  $p$ -nearest-neighbor algorithm that connects the sample with its top  $p$

nearest samples with nonnegative weights to measure their similarities, and assigns 0 to the non-connect samples. This method may not perform well as it is not robust to various types of noise [18]. To solve this problem, many advanced graph construction methods were proposed [18], [19], [20], [21], [22], [23], [23], [3]. See the detailed review in Section II-B. Generally, given the constructed graph, graph-based clustering needs two extra steps to complete the clustering task, i.e., *i*) embed the graph into a low-dimensional space (like spectral embedding), and *ii*) divide the embeddings into different clusters through post-processing like K-means. *The question then arises: does the constructed graph always fit the requirements for the subsequent partition task? The answer is no!*

In this paper, we study a joint learning model that can simultaneously construct the graph and divide the data into different clusters. When optimizing the proposed joint model, the tasks of the graph construction and data partition can well communicate with each other to achieve mutual refinement. Therefore, the resulting graph is tailored to the clustering task. It is also worth pointing out that using a joint optimization framework to deal with two correlated tasks has proven to be effective in many works [3], [24], [25], [26], [27], [28], [29], [28]. Specifically, the constructed graph by our method explores information from the following three aspects: *i*) the initial similarity graph, which is practical in many applications; *ii*), the input data, which contain rich information; and *iii*), the clustering result, which is more discriminative than the input data. The proposed model is finally formulated as a nonnegative and off-diagonal<sup>1</sup> constrained optimization problem, which can be solved efficiently in an iterative manner with convergence guaranteed. By comparing the proposed model with 19 state-of-the-art clustering methods on 10 widely used datasets with 4 clustering metrics, the advantage of the proposed model is validated. In addition, the improvement of the proposed model is confirmed by the Wilcoxon rank sum test with a significance level of 0.05.

The main contributions of this paper are summarized as follows.

1. The proposed method simultaneously learns a cluster membership matrix and an affinity graph, which can exploit the mutual enhancement relation between the two separate steps and lead to a more global solution.
2. The proposed optimization algorithm has the following theoretical guarantees: *i*) the constraints in the proposed

<sup>1</sup>The learned similarity matrix should be an off-diagonal matrix to avoid the trivial solution.

Y. Jia and H. Liu are with the Department of Computer Science, City University of Hong Kong, Kowloon, Hong Kong, (e-mail: yuheng.jia@my.cityu.edu.hk; hliu99-c@my.cityu.edu.hk).

J. Hou and S. Kwong are with the Department of Computer Science, City University of Hong Kong, Kowloon, Hong Kong and also with the City University of Hong Kong Shenzhen Research Institute, Shenzhen, 51800, China, (e-mail: jh.hou@cityu.edu.hk; cssamk@cityu.edu.hk).

This work was supported in part by the Natural Science Foundation of China under Grants 61772344, 61672443, 61873142 and in part by Hong Kong RGC General Research Funds 9042489 (CityU 11206317), 9042322 (CityU 11200116), and Early Career Scheme Funds 9048123 (CityU 21211518).

model can be naturally satisfied<sup>2</sup> in the optimization process; and *ii*) each iteration can decrease the objective function to converge.

The rest of this paper is organized as follows. In Section II, we discuss the related works. Section III presents the proposed model, the optimization algorithm, and its computational complexity analysis and theoretical guarantees. Experimental comparisons and analyses are shown in Section IV, and finally Section V concludes this paper.

## II. RELATED WORK

### A. Notation

Throughout this paper, matrices are denoted by bold uppercase letters, e.g.,  $\mathbf{A}$ , and the element at the  $i$ th row and  $j$ th column of  $\mathbf{A}$  is denoted as  $\mathbf{A}_{ij}$  or  $a_{ij}$ . Vectors are represented by bold lowercase letters, e.g.,  $\mathbf{a}$  and scalars are represented by italic lowercase letters, e.g.,  $a$ . Moreover,  $\top$  stands for the transpose of a matrix,  $\|\mathbf{A}\|_F = \sqrt{\sum_i \sum_j \mathbf{A}_{ij}^2}$  is the Frobenius norm of matrix  $\mathbf{A}$ ,  $\|\mathbf{A}\|_\infty = \max_{ij} |\mathbf{A}_{ij}|$  returns the maximum absolute value of matrix  $\mathbf{A}$ ,  $\text{diag}(\cdot)$  returns the diagonal elements of a matrix as a vector,  $\odot$  returns the Hadamard product of two matrices, i.e., the element-wise multiplication of two matrices,  $\exp(\cdot)$  returns the exponential value,  $\langle \cdot, \cdot \rangle$  calculates the inner product of two matrices,  $\mathbf{I}_k$  denotes an identity matrix of size  $k \times k$ , and  $\mathbf{A} \geq 0$  means each element of  $\mathbf{A}$  is not less than 0, i.e.,  $\mathbf{A}_{ij} \geq 0, \forall i, j$ .  $\mathbf{X} = \{\mathbf{x}_1, \mathbf{x}_2, \dots, \mathbf{x}_n\} \in \mathbb{R}^{d \times n}$  denotes the input data,  $\mathbf{x}_i \in \mathbb{R}^{d \times 1}$  is the  $i$ th sample;  $n$ ,  $d$ , and  $c$  represent the number of samples, the dimension of features, and the number of classes, respectively.

### B. Graph-based Clustering

Different from traditional clustering methods (e.g., K-means) that partition the raw features  $\mathbf{X}$  straightforwardly, graph-based clustering [15], [13] transforms data clustering as a graph partition problem. Specifically, a typical graph-based clustering method is composed of the following steps:

1. Given  $\mathbf{X}$ , generate an affinity matrix  $\mathbf{G} \in \mathbb{R}^{n \times n}$  to represent  $\mathbf{X}$ , where the entries in  $\mathbf{G}$  denote the similarities between the corresponding samples.
2. Decompose the normalized affinity matrix  $\mathbf{W} \in \mathbb{R}^{n \times n}$  to generate the low-dimensional embeddings<sup>3</sup>.
3. Obtain the cluster indicator matrix according to the embeddings.

In the following, we will briefly discuss the widely used approaches for each step.

1) *Graph construction*: The most widely used graph is  $p$ -nearest-neighbor ( $p$ NN) graph [30] that only connects a specified sample with its top  $p$  nearest samples under some distance metrics. Specifically,

$$\mathbf{G}_{ij} = \begin{cases} \mathcal{G}_{ij} & \mathbf{x}_j \in \mathcal{P}(\mathbf{x}_i) \\ 0 & \text{otherwise,} \end{cases} \quad (1)$$

<sup>2</sup>i.e., non-negativity for all the variables and off-diagonal for the similarity matrix.

<sup>3</sup>It is known that a normalized affinity matrix  $\mathbf{W} \in \mathbb{R}^{n \times n}$  usually can achieve better performance than  $\mathbf{G}$  [13], [15], [30]. See the analysis about how to normalize  $\mathbf{G}$  at [30].

where  $\mathcal{P}(\mathbf{x}_i)$  indicates the top  $p$  nearest samples of  $\mathbf{x}_i$ , and  $\mathcal{G}_{ij}$  is the weight between  $\mathbf{x}_i$  and  $\mathbf{x}_j$ . The binary weighting strategy simply sets  $\mathcal{G}_{ij} = 1$  for the connected samples. Another weighting strategy is to use the radial basis function kernel (RBF), i.e.,

$$\mathcal{G}_{ij} = \exp\left(-\frac{\|\mathbf{x}_i - \mathbf{x}_j\|^2}{\sigma^2}\right), \quad (2)$$

to measure the similarities between the samples, where  $\sigma^2$  is the bandwidth of the RBF kernel. Another widely used graph construction method is  $\epsilon$ -neighborhood graph that connects a certain sample with other samples within a ball of radius  $\epsilon$ .

Both  $p$ NN and  $\epsilon$ -neighborhood graphs are sensitive to outliers and noise. To overcome this drawback, many advanced learning methods were proposed to construct the weight matrix of the graph recently. For example, Cheng *et al.* [18] proposed to learn an  $\ell_1$  graph based on the sparsity property of the  $\ell_1$  norm. Nie *et al.* [22] proposed to learn the neighbors adaptively. Dong *et al.* [23], [31] constructed the graph from the perspective of graph signal processing [32]. The smoothness prior is also investigated in graph construction [33], [34]. Wu *et al.* [3] constructed a discriminative graph with the guidance of the supervisory information. Moreover, many models build the affinity graph by the self-representative property of the input data [19], [20], [21].

2) *Low-dimensional embedding*: Given  $\mathbf{W}$ , graph-based clustering decomposes  $\mathbf{W}$  to generate a lower-dimensional embedding. For example, SC [13] is formulated as

$$\min_{\mathbf{V}} \|\mathbf{W} - \mathbf{V}\mathbf{V}^\top\|_F^2, \text{ s.t., } \mathbf{V}^\top \mathbf{V} = \mathbf{I}_k, \quad (3)$$

where  $\mathbf{V} \in \mathbb{R}^{n \times k}$  is the dimension-reduced embedding and can be calculated by the spectral decomposition of  $\mathbf{W}$ . As an alternative, SymNMF [16], [15] decomposes the affinity matrix to be the product of a nonnegative matrix and its transpose,

$$\min_{\mathbf{V}} \|\mathbf{W} - \mathbf{V}\mathbf{V}^\top\|_F^2, \text{ s.t., } \mathbf{V} \geq 0, \quad (4)$$

to produce the lower-dimensional embedding. Other advanced methods like sparse SC (SSC) [35] seeks a block diagonal appearance of  $\mathbf{V}\mathbf{V}^\top$ , and nonnegative spectral clustering [14] generates an orthogonal nonnegative embedding.

3) *Generation of the clustering indicator matrix*: Since the lower-dimensional embedding in graph-based clustering usually cannot indicate the cluster membership, traditionally post-processing like K-means should be carried out to obtain the final clustering result. As a special case, SymNMF generates a nonnegative embedding and the position of the largest value in the  $i$ th row indicates the cluster membership of  $\mathbf{x}_i$ .

## III. PROPOSED MODEL

### A. Model Formulation

As aforementioned, the quality of the graph determines the clustering performance of a graph-based clustering method seriously. However, the existing graph-based clustering methods usually first construct a graph, and then partition it to generate the clustering result with extra processes. It is not clear whether the constructed graph fits the partitioning or not?

In other words, the graph construction methods of existing graph-based clustering methods are not specifically designed with a clustering-purpose, which may lead to compromised clustering performance.

To this end, we propose a clustering-aware graph construction model, which can learn an adaptive graph and generate the clustering result simultaneously. Along with optimizing the proposed joint model, the constructed graph is able to fit the clustering task. Specifically, the proposed model is mathematically formulated as:

$$\begin{aligned} \min_{\mathbf{V}, \mathbf{S}} \alpha \|\mathbf{X} - \mathbf{X}\mathbf{S}\|_F^2 + \|\mathbf{S} - \mathbf{V}\mathbf{V}^\top\|_F^2 + \beta \|\mathbf{S} - \mathbf{W}\|_F^2 \\ \text{s.t.}, \mathbf{V} \geq 0, \mathbf{S} \geq 0, \text{diag}(\mathbf{S}) = 0, \end{aligned} \quad (5)$$

where  $\mathbf{S} \in \mathbb{R}^{n \times n}$  is the adaptive similarity matrix,  $\mathbf{V} \in \mathbb{R}^{n \times c}$  is the clustering indicator matrix with  $c$  being the number of classes,  $\mathbf{W}$  is the initial normalized affinity matrix via a typical graph reconstruction algorithm, and  $\alpha \geq 0, \beta \geq 0$  are two hyper-parameters to balance the contributions of different terms. In what follows, we will explain the proposed model in detail.

The first term  $\|\mathbf{X} - \mathbf{X}\mathbf{S}\|_F^2$  as well as the constraints  $\mathbf{S} \geq 0$ , and  $\text{diag}(\mathbf{S}) = 0$  explores the relationship between samples with a self-expressive manner,  $\text{diag}(\mathbf{S}) = 0$  removes the trivial solution, i.e.,  $\mathbf{S} = \mathbf{I}_n$ , and  $\mathbf{S} \geq 0$  guarantees that the learned weight matrix  $\mathbf{S}$  is a valid similarity matrix. In addition, it has been theoretically proven that a self-expressive model has the property of intra-subspace projection dominance (IPD) [21], i.e., the coefficients over intra subspaces data points are larger than those over inter subspace data points. Based on IPD, it is expected that  $\mathbf{S}_{ij}$  for samples from the same subspace will have larger values.

From the forward perspective, the second term  $\|\mathbf{S} - \mathbf{V}\mathbf{V}^\top\|_F^2$  with the nonnegative constraint  $\mathbf{V} \geq 0$  is responsible for generating the clustering result. That is, assuming  $\mathbf{S}$  is available, the position of the largest value in  $i$ th row of the decomposed  $\mathbf{V}$  indicates the cluster membership of  $\mathbf{x}_i, i \in \{1, \dots, n\}$  like SymNMF. From the backward perspective, the clustering result  $\mathbf{V}$  will be beneficial to the learning of the unknown similarity matrix  $\mathbf{S}$ . That is, the nonnegative constraint on  $\mathbf{V}$  makes the rows of the resulting  $\mathbf{V}$ , which are the low-dimensional representations of input samples, to be more discriminative, and the inner product  $\mathbf{V}\mathbf{V}^\top$  can indicate the similarity between samples precisely, which is further propagated to  $\mathbf{S}$  by minimizing the second term. Moreover, for an ideal similarity matrix, we have

$$\mathbf{S}_{ij} = \begin{cases} 1, & \text{if } l(\mathbf{x}_i) = l(\mathbf{x}_j) \\ 0, & \text{if } l(\mathbf{x}_i) \neq l(\mathbf{x}_j), \end{cases} \quad (6)$$

where  $l(\mathbf{x}_i)$  returns the ground-truth label of  $\mathbf{x}_i$ . It is clear that the ideal similarity matrix is block diagonal and low rank. Minimizing the second term will also seek the low-rankness of  $\mathbf{S}$  to pursue the ideal appearance, since the rank of  $\mathbf{V}\mathbf{V}^\top$  is no greater than  $c$ . Such a bi-directional strategy is different from the traditional forward graph-based clustering methods, which overlook the information from clustering result in graph construction.

The third term has two functions: *i*) it approximates the initial graph which is usually useful in practical applications, and *ii*) it serves as an  $\ell_2$  regularization prior, which encourages the self-expressive term to produce more connections between data samples [36].

When optimizing Eq. (5) iteratively, the clustering result can generate valuable discriminative information and give feedback to guide the construction of the similarity graph. Therefore, the learned graph is tailored to the clustering task. Moreover, since  $\mathbf{V}$  is nonnegative, our model is able to generate the clustering indicator without extra post-processing like K-means.

## B. Optimization Method

To solve Eq. (5), we first introduce the Lagrangian function as

$$\mathcal{L}(\mathbf{S}, \mathbf{V}, \Phi, \Psi) = \mathcal{O}(\mathbf{V}, \mathbf{S}) - \langle \Phi, \mathbf{S} \rangle - \langle \Psi, \mathbf{V} \rangle, \quad (7)$$

where  $\Phi \in \mathbb{R}^{n \times n} \geq 0$  and  $\Psi \in \mathbb{R}^{c \times n} \geq 0$  are the Lagrangian multiplier matrices and  $\mathcal{O}(\mathbf{V}, \mathbf{S})$  denotes the objective function in Eq. (5). Following the Karush-Kuhn-Tucker (KKT) conditions, the optimal solution of Eq. (5) also makes the derivatives of  $\mathcal{L}(\mathbf{S}, \mathbf{V}, \Phi, \Psi)$  with respect to (w.r.t.)  $\mathbf{S}$  and  $\mathbf{V}$  to be 0, i.e.,

$$\frac{\partial \mathcal{L}}{\partial \mathbf{S}} = 2(\mathbf{S} - \mathbf{V}\mathbf{V}^\top) + 2\alpha \mathbf{X}^\top (\mathbf{X}\mathbf{S} - \mathbf{X}) + 2\beta(\mathbf{S} - \mathbf{W}) - \Phi = \mathbf{0}, \quad (8)$$

and

$$\frac{\partial \mathcal{L}}{\partial \mathbf{V}} = -2(\mathbf{S}\mathbf{V} + \mathbf{S}^\top \mathbf{V}) + 4\mathbf{V}\mathbf{V}^\top \mathbf{V} - \Psi = \mathbf{0}, \quad (9)$$

where  $\mathbf{0}$  is a zero matrix with proper size. From the KKT complementary slackness conditions  $\Phi_{ij} \mathbf{S}_{ij}^2 = 0$  and  $\Psi_{ij} \mathbf{V}_{ij}^4 = 0, \forall i, j$ , we obtain the following updating equations for  $\mathbf{S}$  and  $\mathbf{V}$ , respectively, i.e.,

$$\mathbf{S}_{ij}^{t+1} = \mathbf{S}_{ij}^t \left( \frac{\left( \mathbf{V}^t \mathbf{V}^{t\top} + \alpha (\mathbf{X}^\top \mathbf{X})^+ + \alpha (\mathbf{X}^\top \mathbf{X})^- \mathbf{S}^t + \beta \mathbf{W} \right)_{ij}}{\left( \mathbf{S}^t + \alpha (\mathbf{X}^\top \mathbf{X})^+ \mathbf{S}^t + \alpha (\mathbf{X}^\top \mathbf{X})^- + \beta \mathbf{S}^t \right)_{ij}} \right)^{\frac{1}{2}},$$

and

$$\mathbf{V}_{ij}^{t+1} = \mathbf{V}_{ij}^t \left( \frac{\left( \mathbf{S}^{t+1} \mathbf{V}^t + \mathbf{S}^{t+1\top} \mathbf{V}^t \right)_{ij}}{\left( 2\mathbf{V}^t \mathbf{V}^{t\top} \mathbf{V}^t \right)_{ij}} \right)^{\frac{1}{4}}. \quad (11)$$

where  $(\mathbf{X}^\top \mathbf{X})^+$  and  $(\mathbf{X}^\top \mathbf{X})^-$  separate the positive and negative elements of  $\mathbf{X}^\top \mathbf{X}^4$ , i.e.,

$$(\mathbf{X}^\top \mathbf{X})^+ = \frac{|\mathbf{X}^\top \mathbf{X}| + \mathbf{X}^\top \mathbf{X}}{2}, \text{ and } (\mathbf{X}^\top \mathbf{X})^- = \frac{|\mathbf{X}^\top \mathbf{X}| - \mathbf{X}^\top \mathbf{X}}{2}, \quad (12)$$

and  $\mathbf{S}^t$  and  $\mathbf{V}^t$  denote the values of  $\mathbf{S}$  and  $\mathbf{V}$  at the  $t$ -th iteration, respectively. The optimization method is summarized in Algorithm 1. The convergence criteria for Algorithm 1 is  $\|\mathbf{V}^{t+1} - \mathbf{V}^t\|_\infty < 10^{-4}$  &  $\|\mathbf{S}^{t+1} - \mathbf{S}^t\|_\infty < 10^{-4}$ , where & is the AND operator. Note that the constraints (i.e.,  $\mathbf{S} \geq 0, \mathbf{V} \geq 0$  and  $\text{diag}(\mathbf{S}) = 0$ ) can be naturally satisfied by the above updating rules. See Section-III-D for the detailed analysis.

<sup>4</sup>As will be shown in Section III-D, this separation guarantees the non-negativity of  $\mathbf{S}$  and  $\mathbf{V}$  in the optimization procedure.

---

**Algorithm 1** Optimization algorithm for solving Eq. (5)

---

**Input:** A predefined weight matrix  $\mathbf{W}$ , the data matrix  $\mathbf{X}$ , and hyper-parameters  $\alpha$  and  $\beta$ ;

**Initialization:** Assign  $\mathbf{V}$  and the off-diagonal elements of  $\mathbf{S}$  with positive random values,  $\text{diag}(\mathbf{S}) = 0$ ;

- 1: **while** not converged **do**
  - 2:   Update  $\mathbf{S}$  with fixed  $\mathbf{V}$  by Eq. (10);
  - 3:   Update  $\mathbf{V}$  with fixed  $\mathbf{S}$  by Eq. (11);
  - 4: **end while**
  - 5: **Return**  $\mathbf{V}$  and  $\mathbf{S}$ .
- 

### C. Computational Complexity

The sizes of  $\mathbf{X}$ ,  $\mathbf{V}$ ,  $\mathbf{S}$ ,  $\mathbf{X}^\top \mathbf{X}^5$  are  $d \times n$ ,  $n \times c$ ,  $n \times n$ ,  $n \times n$ , respectively. The computational complexities for  $\mathbf{V}\mathbf{V}^\top$ ,  $(\mathbf{X}^\top \mathbf{X})^- \mathbf{S}$ ,  $(\mathbf{X}^\top \mathbf{X})^+ \mathbf{S}$ ,  $\mathbf{S}\mathbf{V}$ ,  $\mathbf{S}^\top \mathbf{V}$ ,  $\mathbf{V}\mathbf{V}^\top \mathbf{V}$  are  $O(n^2c)$ ,  $O(n^3)$ ,  $O(n^3)$ ,  $O(n^2c)$ ,  $O(n^2c)$ ,  $O(2c^2n)$ , respectively. Therefore, the computational complexities for step-2 and step-3 of Algorithm 1 are  $O(n^2c + 2n^3)$  and  $O(2n^2c + 2c^2n)$ , respectively. And the overall computational complexity of each iteration of Algorithm 1 is  $O(2n^3 + 3n^2c + 2c^2n)$ .

### D. Convergence Analysis of Algorithm 1

**Theorem 1:** Algorithm 1 has the following properties:

- 1) the objective function decreases (i.e., non-increases) at each iteration, and is lower-bounded, which guarantee the convergence of the objective function;
- 2) when  $\mathbf{V}$  and the off-diagonal elements of  $\mathbf{S}$  (i.e.,  $\{\mathbf{S}_{ij} | \forall i, j, i \neq j\}$ ) are initialized with strictly positive values, i.e.,  $\mathbf{S}_{ij}^0 > 0, \forall i, j, i \neq j$ , and  $\mathbf{V}_{ij}^0 > 0, \forall i, j$ , and the diagonal elements of  $\mathbf{S}$  are initialized with 0, i.e.,  $\mathbf{S}_{ii}^0 = 0, \forall i$ , we have

$$\mathbf{V}_{ij}^t > 0, \forall i, j, t, \text{ and } \begin{cases} \mathbf{S}_{ij}^t > 0, \forall i, j, t, \text{ and } i \neq j \\ \mathbf{S}_{ii}^t = 0, \forall i, t. \end{cases} \quad (13)$$

The detailed proof of **Theorem 1** can be found in the Appendix A.

## IV. EXPERIMENTAL ANALYSIS

In this section, we conducted extensive experiments to validate the effectiveness of the proposed model. Specifically, we compared the proposed model with 19 state-of-the-art methods on 10 commonly used datasets with 4 clustering metrics. Moreover, we adopted the Wilcoxon rank sum test [37] to evaluate the performance of the proposed model with a significance level of 0.05.

### A. Experiment Settings

The 19 methods under comparison are summarized as follows.

- 1, SymNMF [16], [15] is a symmetric low rank decomposition of graph, which can directly produce the clustering result.

<sup>5</sup>Since  $\mathbf{X}^\top \mathbf{X}$  can be computed in advance, it can be regarded as a single matrix in computing the computational complexity of each iteration.

TABLE I  
Descriptions of Employed Datasets

Dataset	# Samples ( $n$ )	# Classes ( $c$ )	# Dimensions ( $d$ )
SPYBEAN	683	19	35
ECOIL	336	7	8
LIBRAS	360	15	90
YEAST	1484	10	8
IONSPHERE	351	2	34
BINALPHA	1404	36	320
IRIS	150	4	3
WINE	178	3	13
ISOLET	1560	26	617
MSRA	1799	12	256

- 2, SC is a graph-based clustering method based on spectral decomposition. In this paper, we adopted the SC method presented in [13].
- 3, SSC [35] is a convex formulation of SC with a sparse regularizer.
- 4, PCA is a linear dimensionality reduction method.
- 5, RPCA [38], [39] solves a convex optimization problem that is more robust to noise and outliers than the traditional PCA.
- 6, GLPCA [40] is a kind of PCA with a nonlinear graph regularization.
- 7, NMF [41] is a linear dimensionality reduction method that decomposes a nonnegative matrix into two nonnegative matrices with smaller sizes.
- 8, GNMF [42] is an NMF model with graph regularization.
- 9, GMF [43] is a graph regularized low rank matrix approximation method.
- 10, GRPCA [44] is a graph regularized robust PCA method.
- 11, K-means is a basic clustering method.
- 12, LRR [19], [45] is subspace clustering method with a low rank constraint on the coefficient matrix.
- 13, L2-Graph [21] is subspace clustering method with a Frobenius norm on the coefficient matrix.
- 14, CAN [22] is a SC method with a learned graph according to the raw features.
- 15, RSS [46] simultaneously learns an affinity matrix and a subspace coefficient matrix. RSSA uses the affinity matrix to build the graph.
- 16, RSSR [46] uses the coefficient matrix to build the graph.
- 17, RSSAR [46] adopts both the affinity matrix and coefficient matrix to construct the graph.
- 18, CGL [47] learns a graph under the connectivity, sparsity and Laplacian constraints.
- 19, To evaluate the effectiveness of the joint manner of graph construction and clustering, we made up a model termed L2-SymNMF that first builds an L2-Graph, then applies SymNMF on that graph to produce the clustering result.

For all the methods involving a graph structure, we adopted the same  $p$ NN graph with the RBF kernel, where  $p$  was set to  $\text{LR}(\log_2 n + 1)$  [30],  $\sigma$  equals to the mean distance between the sample and its  $p$ -nearest-neighbors, and  $\text{LR}(x)$  rounds  $x$

TABLE II  
Clustering Performance on ECOIL

Methods	ACC	NMI	PUR	ARI
CAN	<b>0.693</b> ↓	<b>0.612</b> •	<b>0.824</b> ↓	<b>0.560</b> ↓
GLPCA	0.554 ± 0.067 ↓	<u>0.529 ± 0.035</u> ↓	0.800 ± 0.021 ↓	<u>0.422 ± 0.069</u> ↓
PCA	0.567 ± 0.061 ↓	0.402 ± 0.028 ↓	0.728 ± 0.016 ↓	0.346 ± 0.054 ↓
GMF	0.533 ± 0.055 ↓	0.513 ± 0.025 ↓	0.796 ± 0.027 ↓	0.389 ± 0.057 ↓
GNNMF	<u>0.581 ± 0.056</u> ↓	0.473 ± 0.039 ↓	0.760 ± 0.030 ↓	<u>0.458 ± 0.093</u> ↓
GRPCA	<b>0.651 ± 0.071</b> ↓	<b>0.611 ± 0.043</b> •	<u>0.812 ± 0.022</u> ↓	<b>0.554 ± 0.106</b> •
K-means	0.553 ± 0.067 ↓	<u>0.532 ± 0.032</u> ↓	0.804 ± 0.024 ↓	0.420 ± 0.024 ↓
L2-Graph	0.465 ± 0.032 ↓	0.334 ± 0.017 ↓	0.668 ± 0.019 ↓	0.220 ± 0.034 ↓
L2-SymNMF	0.502 ± 0.032 ↓	0.350 ± 0.015 ↓	0.665 ± 0.019 ↓	0.249 ± 0.0317 ↓
LRR	0.544 ± 0.071 ↓	0.524 ± 0.032 ↓	0.800 ± 0.022 ↓	0.414 ± 0.085 ↓
NMF	0.558 ± 0.054 ↓	0.446 ± 0.034 ↓	0.750 ± 0.026 ↓	0.417 ± 0.026 ↓
RPCA	0.547 ± 0.067 ↓	0.519 ± 0.024 ↓	<u>0.809 ± 0.019</u> ↓	0.405 ± 0.073 ↓
RSSAR	0.507 ± 0.034 ↓	0.431 ± 0.021 ↓	0.761 ± 0.019 ↓	0.315 ± 0.040 ↓
RSSR	0.486 ± 0.027 ↓	0.355 ± 0.015 ↓	0.708 ± 0.015 ↓	0.270 ± 0.021 ↓
RSSA	0.515 ± 0.025 ↓	0.429 ± 0.020 ↓	0.767 ± 0.018 ↓	0.331 ± 0.044 ↓
SC	0.544 ± 0.044 ↓	0.508 ± 0.029 ↓	<b>0.818 ± 0.024</b> ↓	0.381 ± 0.024 ↓
SSC	<u>0.601 ± 0.036</u> ↓	0.492 ± 0.034 ↓	0.797 ± 0.037 ↓	0.357 ± 0.054 ↓
CGL	0.498 ± 0.005 ↓	0.468 ± 0.08 ↓	0.759 ± 0.005 ↓	0.301 ± 0.005 ↓
SymNMF	0.571 ± 0.070 ↓	0.506 ± 0.055 ↓	0.761 ± 0.056 ↓	0.401 ± 0.056 ↓
<b>Proposed</b>	0.735 ± 0.094	0.626 ± 0.046	0.836 ± 0.019	0.632 ± 0.130

The highest value is highlighted by gray, the second and third highest values are marked by bold, and the fourth and the fifth highest values are underlined. ↓ and ◇ indicate the proposed method is significantly better/worse, respectively, than the compared methods according to the Wilcoxon rank sum test. Moreover, • means there is no significant difference between the proposed model and the compared methods.

to the next smaller integer. For all the methods, the hyper-parameters were determined via exhaustive searching from {0.01, 0.1, 1, 10, 100, 1000} for fair comparisons. For all the graph learning methods like LLR and L2-Graph, a standard SC [13] was adopted to produce the clustering result. For all the data representation methods and SC-based methods, K-means was performed on the low-dimensional embeddings to generate the final clustering result. To exclude the influence of the randomness on K-means and initialization, we repeated each methods 20 times and reported the mean values with standard deviations.

Clustering results were evaluated by four commonly used metrics: clustering accuracy (ACC) [48], normalized mutual information (NMI) [48], purity (PUR) and adjust rand index (ARI). ACC, NMI and PUR all lay in the range of [0, 1], while ARI lays in the range of [-1, 1]. A larger value indicates better clustering performance for all the metrics.

We selected 10 datasets to evaluate the performance of different methods. The number of samples varies from hundreds to thousands and the number of classes varies from 2 to 36. See the detailed information about those datasets from Table I.

### B. Clustering Performance Analysis

Tables II-XI show the clustering performance of different methods, and Tables XII-XIII summarize the overall performance of the proposed model on all the datasets. From those tables, we have the following conclusions.

- 1) The proposed model always has higher ACC/NMI/PUR/ARI than SymNMF over all the datasets. Especially, on IRIS, the ACC increases more

TABLE III  
Clustering Performance on YEAST

Methods	ACC	NMI	PUR	ARI
CAN	<u>0.4218</u> ↓	0.1451 ↓	0.4299 ↓	0.0848 ↓
GLPCA	0.378 ± 0.024 ↓	0.248 ± 0.012 ↓	<u>0.532 ± 0.011</u> ◇	0.148 ± 0.010 ↓
PCA	0.359 ± 0.019 ↓	0.233 ± 0.013 ↓	0.498 ± 0.023 ↓	0.134 ± 0.013 ↓
GMF	0.366 ± 0.025 ↓	0.239 ± 0.008 ↓	0.520 ± 0.006 ◇	0.138 ± 0.008 ↓
GNNMF	0.323 ± 0.0322 ↓	0.190 ± 0.0294 ↓	0.466 ± 0.0211 ↓	0.101 ± 0.0266 ↓
GRPCA	<b>0.451 ± 0.035</b> •	<b>0.260 ± 0.031</b> •	<b>0.535 ± 0.009</b> •	<b>0.171 ± 0.031</b> •
K-means	0.378 ± 0.024 ↓	<u>0.249 ± 0.015</u> ↓	0.531 ± 0.013 ◇	0.148 ± 0.013 ↓
L2-Graph	0.358 ± 0.015 ↓	0.208 ± 0.007 ↓	0.502 ± 0.004 ↓	0.118 ± 0.008 ↓
L2-SymNMF	0.361 ± 0.021 ↓	0.222 ± 0.009 ↓	0.490 ± 0.013 ↓	0.123 ± 0.013 ↓
LRR	0.381 ± 0.022 ↓	<u>0.251 ± 0.006</u> ↓	<u>0.532 ± 0.010</u> ◇	0.150 ± 0.007 ↓
NMF	0.334 ± 0.027 ↓	0.203 ± 0.024 ↓	0.484 ± 0.024 ↓	0.113 ± 0.024 ↓
RPCA	0.384 ± 0.021 ↓	<u>0.249 ± 0.009</u> ↓	<u>0.532 ± 0.013</u> ◇	0.150 ± 0.009 ↓
RSSAR	0.331 ± 0.010 ↓	0.211 ± 0.007 ↓	0.510 ± 0.004 ↓	0.122 ± 0.006 ↓
RSSR	0.333 ± 0.016 ↓	0.208 ± 0.008 ↓	0.511 ± 0.004 ↓	0.118 ± 0.007 ↓
RSSA	0.327 ± 0.014 ↓	0.210 ± 0.004 ↓	0.512 ± 0.002 ↓	0.116 ± 0.004 ↓
SC	0.360 ± 0.011 ↓	0.245 ± 0.007 ↓	<b>0.535 ± 0.008</b> ◇	<u>0.151 ± 0.008</u> ↓
SSC	0.383 ± 0.021 ↓	<u>0.249 ± 0.012</u> ↓	0.527 ± 0.010•	0.149 ± 0.010 ↓
CGL	<b>0.457 ± 0.022</b> •	<u>0.387 ± 0.013</u> ◇	<u>0.662 ± 0.014</u> ◇	<u>0.266 ± 0.019</u> ◇
SymNMF	0.404 ± 0.045 ↓	0.208 ± 0.040 ↓	0.426 ± 0.037 ↓	0.152 ± 0.037 ↓
<b>Proposed</b>	0.467 ± 0.048	<b>0.273 ± 0.021</b>	0.518 ± 0.019	<b>0.186 ± 0.048</b>

TABLE IV  
Clustering Performance on IONSPHERE

Methods	ACC	NMI	PUR	ARI
CAN	0.547 ↓	0.054 ↓	0.641 ↓	-0.0455 ↓
GLPCA	0.658 ± 0.001 ↓	0.139 ± 0.074 ↓	0.675 ± 0.026 ↓	0.095 ± 0.001 ↓
PCA	0.514 ± 0.0035 ↓	0.021 ± 0.0051 ↓	0.641 ± 0 ↓	-0.026 ± 0.0018 ↓
GMF	0.704 ± 0.024 ↓	0.104 ± 0.007 ↓	0.704 ± 0.024 ↓	0.135 ± 0 ↓
GNNMF	—	—	—	—
GRPCA	<b>0.727 ± 0.032</b> ↓	<u>0.149 ± 0.056</u> ↓	<b>0.727 ± 0.032</b> ↓	<b>0.177 ± 0</b> ↓
K-means	0.708 ± 0.015 ↓	0.124 ± 0.028 ↓	0.708 ± 0.015 ↓	0.167 ± 0.015 ↓
L2-Graph	0.555 ± 0 ↓	<u>0.153 ± 0</u> ↓	0.641 ± 0 ↓	-0.017 ± 0.002 ↓
L2-SymNMF	0.671 ± 0.106 ↓	<b>0.199 ± 0.109</b> •	0.706 ± 0.061 ↓	0.145 ± 0.146 ↓
LRR	<u>0.711 ± 0.001</u> ↓	0.130 ± 0.001 ↓	<u>0.711 ± 0.001</u> ↓	<u>0.176 ± 0.002</u> ↓
NMF	—	—	—	—
RPCA	<u>0.711 ± 0.001</u> ↓	0.130 ± 0.001 ↓	<u>0.711 ± 0.001</u> ↓	<u>0.176 ± 0.002</u> ↓
RSSRA	0.529 ± 0 ↓	0.131 ± 0 ↓	0.641 ± 0 ↓	-0.0336 ± 0 ↓
RSSR	0.555 ± 0 ↓	0.117 ± 0 ↓	0.641 ± 0 ↓	-0.016 ± 0 ↓
RSSA	0.529 ± 0 ↓	0.131 ± 0 ↓	0.641 ± 0 ↓	-0.033 ± 0 ↓
SC	0.643 ± 0 ↓	0.046 ± 0 ↓	0.643 ± 0 ↓	0.077 ± 0 ↓
SSC	<b>0.766 ± 0</b> ↓	<b>0.205 ± 0</b> ↓	<b>0.766 ± 0</b> ↓	<b>0.281 ± 0</b> ↓
CGL	0.661 ± 0.000 ↓	0.066 ± 0.000 ↓	0.661 ± 0.000 ↓	0.100 ± 0.000 ↓
SymNMF	0.652 ± 0.080 ↓	0.111 ± 0.071 ↓	0.679 ± 0.051 ↓	0.110 ± 0.051 ↓
<b>Proposed</b>	0.787 ± 0.066	0.256 ± 0.065	0.790 ± 0.056	0.339 ± 0.123

TABLE V  
Clustering Performance on BINALPHA

Methods	ACC	NMI	PUR	ARI
CAN	0.332 ↓	0.445 ↓	0.363 ↓	0.091 ↓
GLPCA	0.409 ± 0.022 ↓	0.570 ± 0.010 ↓	0.439 ± 0.018 ↓	0.268 ± 0.015 ↓
PCA	0.352 ± 0.022 ↓	0.512 ± 0.015 ↓	0.376 ± 0.021 ↓	0.210 ± 0.017 ↓
GMF	0.449 ± 0.016 ↓	0.606 ± 0.008 ↓	0.487 ± 0.015 ↓	0.307 ± 0.013 ↓
GNNMF	0.366 ± 0.018 ↓	0.523 ± 0.013 ↓	0.392 ± 0.017 ↓	0.218 ± 0.014 ↓
GRPCA	0.458 ± 0.020 ↓	<b>0.619 ± 0.009</b> •	0.490 ± 0.017 ↓	<u>0.328 ± 0.012</u> ↓
K-means	0.394 ± 0.015 ↓	0.564 ± 0.010 ↓	0.425 ± 0.016 ↓	0.259 ± 0.016 ↓
L2-Graph	0.345 ± 0.010 ↓	0.481 ± 0.007 ↓	0.374 ± 0.009 ↓	0.192 ± 0.008 ↓
L2-SymNMF	0.312 ± 0.013 ↓	0.452 ± 0.008 ↓	0.352 ± 0.012 ↓	0.172 ± 0.009 ↓
LLR	0.414 ± 0.025 ↓	0.573 ± 0.010 ↓	0.443 ± 0.022 ↓	0.272 ± 0.015 ↓
NMF	0.357 ± 0.017 ↓	0.518 ± 0.013 ↓	0.386 ± 0.017 ↓	0.211 ± 0.017 ↓
RPCA	0.412 ± 0.017 ↓	0.572 ± 0.008 ↓	0.442 ± 0.014 ↓	0.273 ± 0.016 ↓
RSSAR	0.121 ± 0.004 ↓	0.185 ± 0.006 ↓	0.131 ± 0.003 ↓	0.023 ± 0.004 ↓
RSSR	0.203 ± 0.011 ↓	0.309 ± 0.006 ↓	0.216 ± 0.010 ↓	0.075 ± 0.005 ↓
RSSA	0.116 ± 0.003 ↓	0.185 ± 0.007 ↓	0.124 ± 0.003 ↓	0.014 ± 0.002 ↓
SC	<b>0.477 ± 0.018</b> •	<u>0.615 ± 0.008</u> ↓	<b>0.506 ± 0.014</b> ↓	<b>0.329 ± 0.014</b> ↓
SSC	<b>0.466 ± 0.020</b> ↓	0.613 ± 0.010 ↓	<u>0.501 ± 0.018</u> ↓	<u>0.327 ± 0.016</u> ↓
CGL	<u>0.467 ± 0.018</u> ↓	<u>0.615 ± 0.006</u> ↓	<u>0.502 ± 0.012</u> ↓	0.320 ± 0.010 ↓
SymNMF	0.465 ± 0.019 ↓	<b>0.619 ± 0.009</b> •	<b>0.504 ± 0.016</b> ↓	<b>0.335 ± 0.016</b> •
<b>Proposed</b>	0.484 ± 0.018	0.622 ± 0.010	0.516 ± 0.017	0.337 ± 0.015

TABLE VI  
Clustering Performance on IRIS

Methods	ACC	NMI	PUR	ARI
CAN	0.693 ↓	0.596 ↓	0.693 ↓	0.560 ↓
GLPCA	0.520 ± 0.083 ↓	0.228 ± 0.014 ↓	0.556 ± 0.042 ↓	0.148 ± 0.137 ↓
PCA	0.722 ± 0.121 ↓	0.597 ± 0.011 ↓	0.760 ± 0.062 ↓	0.528 ± 0.053 ↓
GMF	0.821 ± 0.141 ↓	0.704 ± 0.089 ↓	0.845 ± 0.091 ↓	0.663 ± 0.125 ↓
GNMF	0.776 ± 0.067 ↓	0.626 ± 0.034 ↓	0.780 ± 0.057 ↓	0.567 ± 0.053 ↓
GRPCA	<b>0.884 ± 0.085●</b>	<b>0.781 ± 0.047●</b>	<b>0.892 ± 0.053●</b>	<b>0.737 ± 0.070●</b>
K-means	0.757 ± 0.183 ↓	0.668 ± 0.101 ↓	0.811 ± 0.108 ↓	0.615 ± 0.108 ↓
L2-Graph	0.830 ± 0.019 ↓	0.663 ± 0.015 ↓	0.830 ± 0.019 ↓	0.621 ± 0.022 ↓
L2-SymNMF	0.807 ± 0.006 ↓	0.638 ± 0.026 ↓	0.807 ± 0.006 ↓	0.585 ± 0.009 ↓
LRR	<b>0.852 ± 0.115 ↓</b>	<b>0.722 ± 0.065 ↓</b>	<b>0.867 ± 0.068 ↓</b>	<b>0.693 ± 0.093 ↓</b>
NMF	0.719 ± 0.112 ↓	0.614 ± 0.098 ↓	0.738 ± 0.087 ↓	0.545 ± 0.087 ↓
RPCA	0.838 ± 0.125 ↓	0.711 ± 0.077 ↓	0.856 ± 0.081 ↓	0.677 ± 0.109 ↓
RSSAR	0.510 ± 0.026 ↓	0.419 ± 0.069 ↓	0.615 ± 0.022 ↓	0.312 ± 0.065 ↓
RSSR	0.826 ± 0 ↓	0.652 ± 0.001 ↓	0.826 ± 0 ↓	0.610 ± 0.001 ↓
RSSA	0.519 ± 0.029 ↓	0.579 ± 0 ↓	0.666 ± 0 ↓	0.442 ± 0.009 ↓
SC	0.461 ± 0.002 ↓	0.298 ± 0.004 ↓	0.561 ± 0.002 ↓	0.187 ± 0.002 ↓
SSC	0.854 ± 0.115 ↓	0.725 ± 0.066 ↓	0.869 ± 0.069 ↓	0.695 ± 0.094 ↓
CGL	<b>0.920 ± 0.000●</b>	<b>0.796 ± 0.000●</b>	<b>0.920 ± 0.000●</b>	<b>0.785 ± 0.000◇</b>
SymNMF	0.665 ± 0.126 ↓	0.417 ± 0.170 ↓	0.681 ± 0.116 ↓	0.384 ± 0.116 ↓
<b>Proposed</b>	<b>0.903 ± 0.005</b>	<b>0.786 ± 0.012</b>	<b>0.903 ± 0.005</b>	<b>0.751 ± 0.011</b>

TABLE VII  
Clustering Performance on WINE

Methods	ACC	NMI	PUR	ARI
CAN	0.668 ↓	0.521 ↓	0.707 ↓	0.490 ↓
GLPCA	0.923 ± 0.005 ↓	0.767 ± 0.012 ↓	0.923 ± 0.005 ↓	0.773 ± 0.015 ↓
PCA	<b>0.929 ± 0.002 ↓</b>	0.764 ± 0.006 ↓	0.929 ± 0.002 ↓	0.789 ± 0.007 ↓
GMF	0.921 ± 0 ↓	0.754 ± 0 ↓	0.921 ± 0 ↓	0.768 ± 0 ↓
GNMF	0.918 ± 0.009 ↓	0.741 ± 0.025 ↓	0.918 ± 0.009 ↓	0.761 ± 0.025 ↓
GRPCA	0.923 ± 0.005 ↓	0.776 ± 0.004 ↓	0.923 ± 0.005 ↓	0.774 ± 0.014 ↓
K-means	0.923 ± 0.005 ↓	0.766 ± 0.011 ↓	0.923 ± 0.005 ↓	0.773 ± 0.005 ↓
L2-Graph	<b>0.946 ± 0.002 ↓</b>	<b>0.808 ± 0.009 ↓</b>	<b>0.946 ± 0.002 ↓</b>	<b>0.837 ± 0.008 ↓</b>
L2-SymNMF	0.874 ± 0.134 ↓	0.713 ± 0.155 ↓	0.881 ± 0.117 ↓	0.722 ± 0.183 ↓
LRR	0.924 ± 0.004 ↓	0.769 ± 0.009 ↓	0.924 ± 0.004 ↓	0.776 ± 0.012 ↓
NMF	0.854 ± 0.107 ↓	0.654 ± 0.129 ↓	0.857 ± 0.099 ↓	0.648 ± 0.099 ↓
RPCA	0.926 ± 0.008 ↓	0.779 ± 0.024 ↓	0.926 ± 0.008 ↓	0.782 ± 0.022 ↓
RSSAR	0.927 ± 0.088 ↓	0.797 ± 0.075 ↓	0.930 ± 0.073 ↓	0.817 ± 0.103 ↓
RSSR	<b>0.935 ± 0.002 ↓</b>	<b>0.801 ± 0.006 ↓</b>	<b>0.935 ± 0.002 ↓</b>	<b>0.809 ± 0.007 ↓</b>
RSSA	0.921 ± 0 ↓	0.741 ± 0 ↓	0.921 ± 0 ↓	0.770 ± 0 ↓
SC	<b>0.949 ± 0 ↓</b>	<b>0.829 ± 0 ↓</b>	<b>0.949 ± 0 ↓</b>	<b>0.848 ± 0 ↓</b>
SSC	0.903 ± 0.088 ↓	0.766 ± 0.086 ↓	0.909 ± 0.070 ↓	0.765 ± 0.105 ↓
CGL	0.902 ± 0.003 ↓	0.705 ± 0.006 ↓	0.902 ± 0.003 ↓	0.719 ± 0.007 ↓
SymNMF	0.852 ± 0.128 ↓	0.667 ± 0.147 ↓	0.856 ± 0.116 ↓	0.667 ± 0.116 ↓
<b>Proposed</b>	0.959 ± 0.004	0.852 ± 0.109	0.959 ± 0.004	0.881 ± 0.127

TABLE VIII  
Clustering Performance on MSRA

Methods	ACC	NMI	PUR	ARI
CAN	0.533 ↓	0.602 ↓	0.537 ↓	0.313 ↓
GLPCA	0.514 ± 0.033 ↓	0.583 ± 0.032 ↓	0.541 ± 0.030 ↓	0.349 ± 0.045 ↓
PCA	0.525 ± 0.030 ↓	0.585 ± 0.029 ↓	0.551 ± 0.027 ↓	0.378 ± 0.041 ↓
GMF	0.495 ± 0.037 ↓	0.553 ± 0.031 ↓	0.522 ± 0.029 ↓	0.324 ± 0.043 ↓
GNMF	0.497 ± 0.034 ↓	0.559 ± 0.032 ↓	0.525 ± 0.029 ↓	0.345 ± 0.036 ↓
GRPCA	0.546 ± 0.049●	<b>0.667 ± 0.034●</b>	0.584 ± 0.041●	<b>0.409 ± 0.044●</b>
K-means	0.497 ± 0.040 ↓	0.573 ± 0.033 ↓	0.529 ± 0.033 ↓	0.342 ± 0.033 ↓
L2-Graph	0.539 ± 0.037●	<b>0.646 ± 0.048 ↓</b>	0.587 ± 0.033●	0.369 ± 0.059 ↓
L2-SymNMF	<b>0.566 ± 0.039●</b>	<b>0.688 ± 0.026◇</b>	<b>0.610 ± 0.031◇</b>	<b>0.463 ± 0.043◇</b>
LRR	0.512 ± 0.034 ↓	0.594 ± 0.031 ↓	0.548 ± 0.027 ↓	0.364 ± 0.041 ↓
NMF	0.484 ± 0.035 ↓	0.539 ± 0.031 ↓	0.507 ± 0.029 ↓	0.321 ± 0.029 ↓
RPCA	0.520 ± 0.036 ↓	0.589 ± 0.029 ↓	0.547 ± 0.027 ↓	0.359 ± 0.032 ↓
RSSAR	<b>0.549 ± 0.041●</b>	0.565 ± 0.020 ↓	<b>0.593 ± 0.031●</b>	0.335 ± 0.042 ↓
RSSR	<b>0.642 ± 0.029◇</b>	<b>0.736 ± 0.027◇</b>	<b>0.690 ± 0.029◇</b>	<b>0.548 ± 0.038◇</b>
RSSA	0.509 ± 0.020 ↓	0.485 ± 0.013 ↓	0.542 ± 0.020 ↓	0.275 ± 0.021 ↓
SC	0.447 ± 0.027 ↓	0.546 ± 0.022 ↓	0.484 ± 0.025 ↓	0.292 ± 0.025 ↓
SSC	0.495 ± 0.046 ↓	0.566 ± 0.039 ↓	0.532 ± 0.042 ↓	0.335 ± 0.049 ↓
CGL	<b>0.559 ± 0.022●</b>	0.641 ± 0.011 ↓	<b>0.595 ± 0.019●</b>	<b>0.427 ± 0.017●</b>
SymNMF	0.457 ± 0.027 ↓	0.569 ± 0.027 ↓	0.502 ± 0.029 ↓	0.333 ± 0.029 ↓
<b>Proposed</b>	<b>0.557 ± 0.045</b>	<b>0.673 ± 0.032</b>	<b>0.588 ± 0.038</b>	<b>0.432 ± 0.041</b>

TABLE IX  
Clustering Performance on ISOLET

Methods	ACC	NMI	PUR	ARI
CAN	0.553 ↓	0.733 ↓	0.590 ↓	0.416 ↓
GLPCA	0.589 ± 0.037 ↓	0.744 ± 0.016 ↓	0.632 ± 0.028 ↓	0.528 ± 0.033 ↓
PCA	<b>0.635 ± 0.047●</b>	<b>0.750 ± 0.024 ↓</b>	<b>0.675 ± 0.040●</b>	<b>0.563 ± 0.035●</b>
GNMF	—	—	—	—
GRPCA	<b>0.593 ± 0.034 ↓</b>	<b>0.752 ± 0.011 ↓</b>	<b>0.633 ± 0.020 ↓</b>	<b>0.540 ± 0.018 ↓</b>
K-means	0.588 ± 0.034 ↓	0.742 ± 0.019 ↓	0.631 ± 0.031 ↓	0.524 ± 0.031 ↓
L2-Graph	0.547 ± 0.036 ↓	0.702 ± 0.016 ↓	0.587 ± 0.026 ↓	0.472 ± 0.033 ↓
L2-SymNMF	0.523 ± 0.019 ↓	0.682 ± 0.014 ↓	0.585 ± 0.018 ↓	0.443 ± 0.024 ↓
LRR	<b>0.601 ± 0.024 ↓</b>	<b>0.749 ± 0.013 ↓</b>	<b>0.639 ± 0.023 ↓</b>	<b>0.536 ± 0.021 ↓</b>
NMF	—	—	—	—
RPCA	<b>0.593 ± 0.026 ↓</b>	0.745 ± 0.012 ↓	0.632 ± 0.024 ↓	0.529 ± 0.027 ↓
RSSAR	0.217 ± 0.006 ↓	0.266 ± 0.004 ↓	0.245 ± 0.004 ↓	0.074 ± 0.003 ↓
RSSR	0.366 ± 0.018 ↓	0.476 ± 0.010 ↓	0.397 ± 0.015 ↓	0.243 ± 0.010 ↓
RSSA	0.221 ± 0.009 ↓	0.224 ± 0.004 ↓	0.254 ± 0.008 ↓	0.072 ± 0.003 ↓
SC	0.583 ± 0.037 ↓	0.743 ± 0.014 ↓	0.620 ± 0.029 ↓	0.512 ± 0.029 ↓
SSC	0.547 ± 0.037 ↓	0.720 ± 0.019 ↓	0.583 ± 0.027 ↓	0.477 ± 0.034 ↓
CGL	0.589 ± 0.000 ↓	0.024 ± 0.000 ↓	0.589 ± 0.000 ↓	0.031 ± 0.000 ↓
SymNMF	0.582 ± 0.023 ↓	<b>0.774 ± 0.010 ↓</b>	<b>0.659 ± 0.017 ↓</b>	0.536 ± 0.017 ↓
<b>Proposed</b>	<b>0.633 ± 0.024</b>	0.781 ± 0.005	0.685 ± 0.014	0.571 ± 0.013

TABLE X  
Clustering Performance on LIBRAS

Methods	ACC	NMI	PUR	ARI
CAN	<b>0.483 ↓</b>	0.654◇	<b>0.525 ↓</b>	0.398●
GLPCA	0.442 ± 0.019 ↓	0.572 ± 0.017 ↓	0.469 ± 0.024 ↓	0.303 ± 0.019 ↓
PCA	0.431 ± 0.022 ↓	0.506 ± 0.018 ↓	0.459 ± 0.019 ↓	0.237 ± 0.020 ↓
GMF	0.445 ± 0.030 ↓	0.577 ± 0.020 ↓	0.479 ± 0.029 ↓	0.303 ± 0.022 ↓
GNMF	0.463 ± 0.028 ↓	0.564 ± 0.030 ↓	0.490 ± 0.023 ↓	0.300 ± 0.034 ↓
GRPCA	0.464 ± 0.033 ↓	0.593 ± 0.027 ↓	0.494 ± 0.027 ↓	0.236 ± 0.031 ↓
K-means	0.435 ± 0.023 ↓	0.562 ± 0.023 ↓	0.464 ± 0.025 ↓	0.293 ± 0.025 ↓
L2-Graph	<b>0.497 ± 0.028●</b>	<b>0.622 ± 0.026 ↓</b>	<b>0.524 ± 0.021●</b>	<b>0.361 ± 0.018 ↓</b>
L2-SymNMF	<b>0.521 ± 0.022◇</b>	<b>0.639 ± 0.018●</b>	<b>0.544 ± 0.016◇</b>	<b>0.383 ± 0.024 ↓</b>
LRR	0.440 ± 0.023 ↓	0.569 ± 0.015 ↓	0.469 ± 0.021 ↓	0.299 ± 0.018 ↓
NMF	0.460 ± 0.032 ↓	0.558 ± 0.024 ↓	0.493 ± 0.025 ↓	0.296 ± 0.025 ↓
RPCA	0.444 ± 0.027 ↓	0.569 ± 0.020 ↓	0.470 ± 0.022 ↓	0.300 ± 0.022 ↓
RSSAR	<b>0.492 ± 0.024●</b>	0.604 ± 0.020 ↓	0.519 ± 0.024●	0.340 ± 0.022 ↓
RSSR	0.476 ± 0.027 ↓	0.574 ± 0.016 ↓	0.506 ± 0.023 ↓	0.314 ± 0.022 ↓
RSSA	0.472 ± 0.024 ↓	0.594 ± 0.015 ↓	0.496 ± 0.016 ↓	0.331 ± 0.020 ↓
SC	0.466 ± 0.030 ↓	0.615 ± 0.023 ↓	0.500 ± 0.025 ↓	0.347 ± 0.025 ↓
SSC	0.457 ± 0.032 ↓	0.600 ± 0.022 ↓	0.495 ± 0.023 ↓	0.336 ± 0.033 ↓
CGL	0.470 ± 0.027 ↓	0.588 ± 0.017 ↓	0.500 ± 0.021 ↓	0.333 ± 0.022 ↓
SymNMF	0.482 ± 0.023 ↓	<b>0.619 ± 0.020 ↓</b>	<b>0.520 ± 0.019 ↓</b>	<b>0.356 ± 0.020 ↓</b>
<b>Proposed</b>	<b>0.501 ± 0.023</b>	<b>0.643 ± 0.012</b>	<b>0.532 ± 0.011</b>	<b>0.397 ± 0.016</b>

TABLE XI  
Clustering Performance on SOYBEAN

Methods	ACC	NMI	PUR	ARI
CAN	0.540 ↓	0.697 ↓	0.638 ↓	0.341 ↓
GLPCA	0.573 ± 0.029 ↓	0.700 ± 0.021 ↓	0.675 ± 0.030 ↓	<b>0.445 ± 0.044●</b>
PCA	0.591 ± 0.035 ↓	0.688 ± 0.022 ↓	0.690 ± 0.029 ↓	<b>0.446 ± 0.048●</b>
GMF	0.551 ± 0.049 ↓	0.689 ± 0.033 ↓	0.667 ± 0.040 ↓	0.420 ± 0.057●
GNMF	<b>0.605 ± 0.039 ↓</b>	<b>0.715 ± 0.021 ↓</b>	<b>0.704 ± 0.026●</b>	<b>0.475 ± 0.045◇</b>
GRPCA	0.576 ± 0.043 ↓	0.710 ± 0.027 ↓	0.676 ± 0.027 ↓	<b>0.445 ± 0.050●</b>
K-means	0.560 ± 0.033 ↓	0.699 ± 0.022 ↓	0.659 ± 0.037 ↓	0.424 ± 0.037●
L2-Graph	0.588 ± 0.026 ↓	<b>0.730 ± 0.018 ↓</b>	0.692 ± 0.026●	0.424 ± 0.025●
L2-SymNMF	<b>0.593 ± 0.042 ↓</b>	<b>0.728 ± 0.027 ↓</b>	0.697 ± 0.031●	0.422 ± 0.045●
LRR	0.566 ± 0.039 ↓	0.698 ± 0.027 ↓	0.666 ± 0.032 ↓	0.439 ± 0.057●
NMF	<b>0.598 ± 0.043 ↓</b>	<b>0.718 ± 0.021 ↓</b>	<b>0.709 ± 0.031●</b>	<b>0.461 ± 0.031◇</b>
RPCA	0.570 ± 0.030 ↓	0.700 ± 0.015 ↓	0.668 ± 0.024	0.435 ± 0.041●
RSSAR	0.573 ± 0.041 ↓	<b>0.715 ± 0.028 ↓</b>	0.693 ± 0.030 ↓	0.442 ± 0.037●
RSSR	0.578 ± 0.053 ↓	0.703 ± 0.014 ↓	0.696 ± 0.037●	0.442 ± 0.034●
RSSA	0.558 ± 0.043 ↓	0.700 ± 0.024 ↓	0.671 ± 0.038 ↓	0.414 ± 0.034●
SC	0.495 ± 0.038 ↓	0.641 ± 0.026 ↓	0.604 ± 0.040 ↓	0.355 ± 0.040 ↓
SSC	0.574 ± 0.031 ↓	0.704 ± 0.020 ↓	0.672 ± 0.031 ↓	0.441 ± 0.038●
CGL	<b>0.593 ± 0.022 ↓</b>	0.712 ± 0.019 ↓	0.680 ± 0.018 ↓	0.441 ± 0.016●
SymNMF	0.513 ± 0.042 ↓	0.664 ± 0.020 ↓	0.620 ± 0.029 ↓	0.326 ± 0.029 ↓
<b>Proposed</b>	<b>0.638 ± 0.025</b>	<b>0.744 ± 0.017</b>	<b>0.713 ± 0.025</b>	<b>0.428 ± 0.050</b>

than 35% compared with SymNMF. Moreover,

TABLE XII  
Rank Counting for the Proposed Method

	Rank 1	Rank 2~3	Rank 4~5	Rank 6~20
Quantity	23/40	13/40	2/40	2/40
Ratio	57.5%	32.5%	5%	5%

TABLE XIII  
Statistics of the Comparison Between the Proposed Method and the Compared Methods in Terms of the Wilcoxon Rank Sum Test

	Significantly better	No significant difference	Significantly worse
Quantity	662/744	60/744	22/744
Ratio	89.0%	8.1%	2.9%

according to the Wilcoxon rank sum test, the improvements under all the cases (40/40) are significant, which validates our basic assumption that the predefined similarity graph is usually not the best choice. By learning a reasonable graph from raw features, the proposed model can generate the graph with higher quality.

- 2) NMF and GNMF require the input data to be nonnegative, so they are not applicable to IONSHPERE and ISOLET due to that IONSHPERE and ISOLET consist of mixed signed data. Although our model also contains the nonnegative constraints on  $\mathbf{S}$  and  $\mathbf{V}$ , it can cope with the mixed sign data by separating the negative and positive components in  $\mathbf{X}^T\mathbf{X}$ . Therefore, our method is more flexible than NMF-like methods.
- 3) SymNMF performs better than SC in most cases (29/40). Taking IRIS as an example, ACC increases 45% and PUR increases 105%. Note that both SymNMF and SC utilize the same predefined graph in the experiments, the advantage of SymNMF over SC validates that directly generating data partition is beneficial to clustering.
- 4) CAN is a graph-based clustering method with an adaptive graph according to the raw features, and SSC is an advanced SC method based on the predefined graph. CAN performs better than SSC on ECOIL, LIBRAS, YEAST and MSRA, while SSC performs better than CAN on IONSHPERE, ISOLET, SOYBEAN, BINALPHA, WINE and IRIS. This phenomenon demonstrates that both the raw features and the predefined graph are important to clustering if they are well exploited.
- 5) Real world datasets usually contain different types of noise and outliers, so the models that are robust to noise and outliers may produce high quality clustering results. For example, the robust models like RPCA and GRPCA get quite well performance on ECOIL, YEAST, IONSPHERE, IRIS, BINAPHPA and ISOLET. Moreover, according to the IPD property of L2 norm [21], the L2-Graph is also robust to noise, which is also applicable to our model.
- 6) The methods with a graph regularizer usually achieve better performance than the original models. For example, GNMF and GMF perform better than NMF and

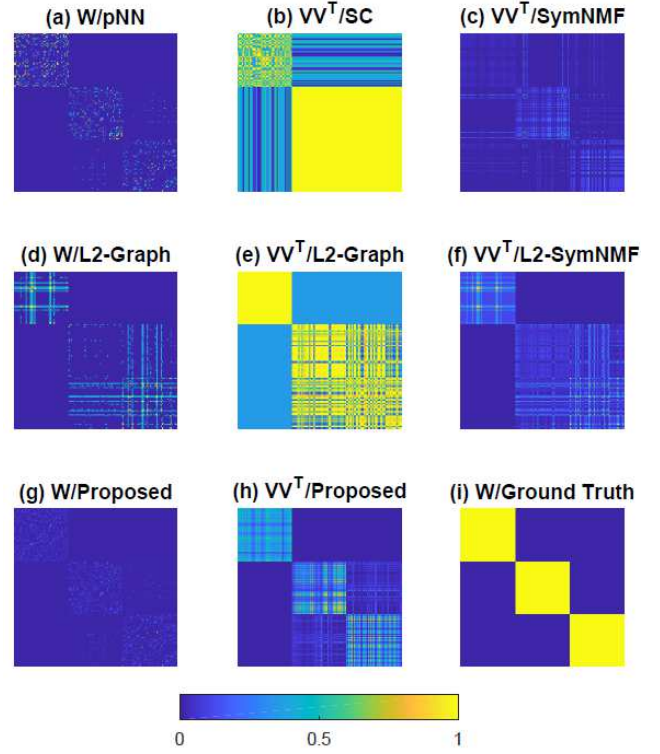


Fig. 1. Visual comparison of the affinity matrices constructed by different methods, and the corresponding  $\mathbf{V}^T\mathbf{V}$  by different methods on the IRIS dataset. (a), (d), (g) and (i) are the affinity matrices built by the  $p$ NN graph, L2-Graph, our method, and the ground truth cluster indicator, respectively. (b), (c), (e), (f) and (h) denote the inner product of the low-dimensional embeddings by SC, SymNMF, L2-Graph, L2-SymNMF, and our method, respectively. All the matrices are normalized to  $[0, 1]$ , and share the same color map.

PCA, respectively. This phenomenon exposes the importance of exploiting the local structures in clustering. Both PCA and NMF can be regarded as the variants of K-means [49], [50] in a soft manner, and the graph regularizer is highly related to spectral clustering [51]. These phenomena suggest that graph-based clustering can usually generate better clustering performance than K-means-like methods.

- 7) The proposed model is significantly better than L2-Graph in most cases (34/40) in accordance with the Wilcoxon rank-sum test. It also obtains better performance than L2-SymNMF in most cases (34/40). Especially, 30 out of 40 cases of them are significantly better. Taking ECOIL as an example, the proposed model generates approximate 50% higher ACC than L2-Graph and L2-SymNMF. Both L2-Graph and L2-SymNMF learn the graph from the raw features with a Frobenius norm on the coefficient matrix like our model. While our method is processed in a joint manner. Those phenomena verify that the constructed graph in our model is more suitable for clustering.
- 8) Table XII summarizes the ranking of the proposed model among all the 20 methods on all the datasets with different metrics. What is noteworthy in Table XII is that the proposed model ranks the first under 23 out of 40 cases (57.5%). Moreover, the proposed model ranks

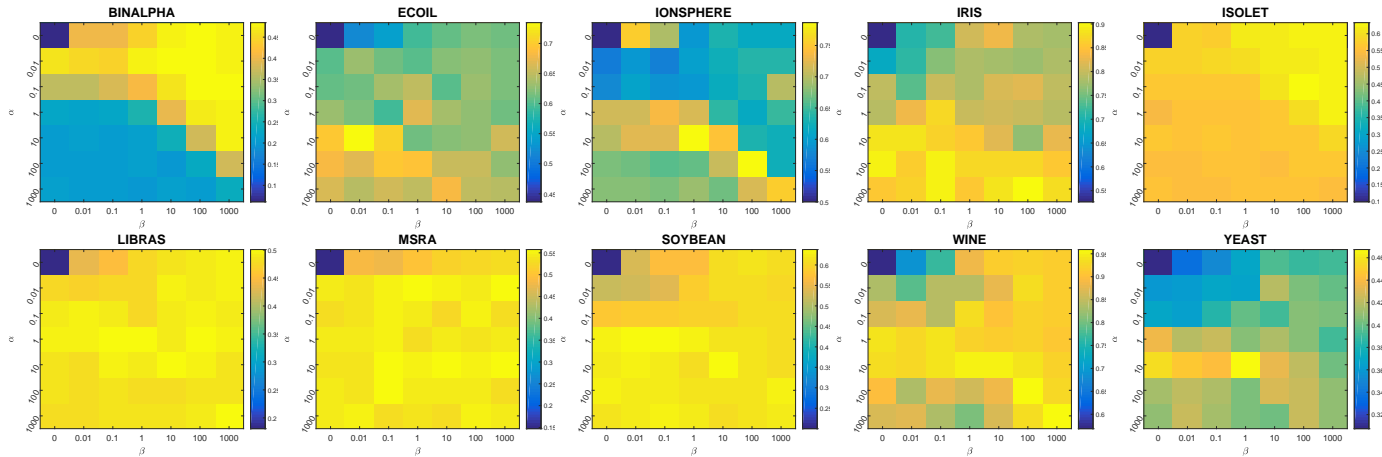


Fig. 2. Clustering ACC of the proposed model versus  $\alpha$  and  $\beta$  on 10 datasets.

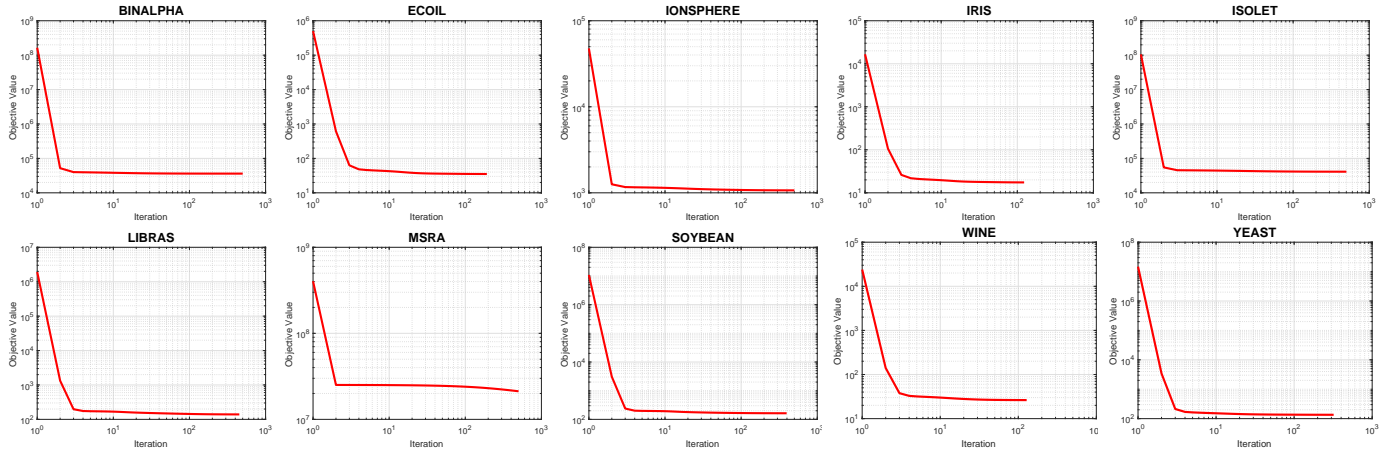


Fig. 3. Illustration of objective values against the number of iteration on 10 datasets.

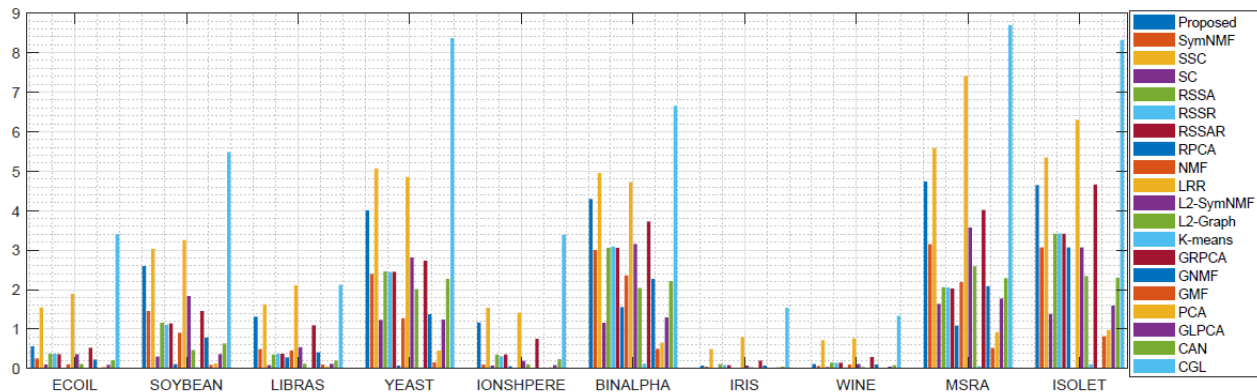


Fig. 4. Illustration of the running time comparison for all the methods on different datasets.

top 3 under 90.0% cases. Table XIII sums up whether the proposed method is significantly better, or worse than the compared methods. It is apparent from Table XIII that the proposed model performs significantly better than the compared methods in approximate 90% of cases; and only in less than 3% of cases that the proposed model gets significantly worse results. The

above analyses support the conclusion that the proposed model produces better clustering performance than the compared 19 models on those 10 datasets.

### C. Visual Comparison of Learned Affinity Matrices

We visually show the affinity matrices constructed by the  $p$ NN graph, the L2-Graph, the proposed method, and the



ground truth relationship on the IRIS dataset in Fig. 1. The IRIS dataset contains three categories, and the second and third categories are quite close to each other, which is challenging to distinguish. Note that the L2-Graph [21] and L2-SymNMF share the same affinity matrix in Fig. 1-(d), while SC [13] and SymNMF [16], [15] share the same affinity matrix in Fig. 1-(a). Since the inner product of the lower-dimensional embeddings  $\mathbf{V}^T\mathbf{V}$  can indicate the similarity relations among samples directly, we also show  $\mathbf{V}^T\mathbf{V}$  for different methods, including SC, SymNMF, L2-Graph, L2-SymNMF and our method.

Compared with the  $p$ NN graph and L2-Graph, the affinity matrix by our model exhibits denser correct connections and a more obvious block diagonal structure. Moreover, SC with the  $p$ NN graph as the affinity matrix cannot distinguish the second category from the third category as shown in Fig. 1-(b). SymNMF performs slightly better than SC; however, there are still many incorrect connections as shown in Fig. 1-(c). In contrast to all the compared methods,  $\mathbf{V}^T\mathbf{V}$  of our method appears a much better block diagonal structure, which visually validates the advantage of our method.

#### D. Parameter Sensitivity Analysis

There are two hyper-parameters in the proposed model, i.e.,  $\alpha$  and  $\beta$  which adjust the contributions to graph construction from the raw features and the predefined graph, respectively. Fig. 2 plots the values of ACC w.r.t. different  $\alpha$  and  $\beta$ , where we can see that

- 1) the highest ACC never occurs when  $\alpha = 0$  or  $\beta = 0$ , which indicates that both  $\alpha$  and  $\beta$  are critical to the proposed model. Moreover, the lowest value always appears when both  $\alpha = 0$  and  $\beta = 0$ . The reason is that, when  $\alpha = \beta = 0$ , no useful information can be transferred to the cluster membership matrix  $\mathbf{V}$ .
- 2) the optimal ACCs of all the datasets usually occur in a common range, i.e.,  $\alpha \in \{0.1, 10\}$ , and  $\beta \in \{1, 100\}$ , which validates the robustness of our model to the hyper-parameters.
- 3) nevertheless, how to adaptively determine the optimal  $\alpha$  and  $\beta$  based on the characteristic of the input data is still a challenging problem. One possible solution is to resort to the methodology of Bayesian inference, which defines an explicit prior probability distribution over  $\alpha$  and  $\beta$ , and then infers them by maximizing the type II likelihood [52], [37].

#### E. Convergence Analysis

The convergence of the proposed optimization algorithm has been theoretically proven in Section III-D. Here, we study its empirical convergence behavior. Specifically, Fig. 3 shows the objective function values according to the iteration number on all the datasets when  $\alpha = 1$  and  $\beta = 1$ , from which we can observe that the values of the objective function decrease monotonically on all the datasets with the increase of the number of iterations, which is consistent with the theoretical analysis. Moreover, on all the datasets the objective values get convergent in approximately 100 iterations, which illustrates the high efficiency of our optimization algorithm.

#### F. Comparison of Running Time

The running time comparisons are shown in Fig. 4 for all the methods. From Fig. 4, we have the following observations.

- 1) The proposed method is usually faster than SSC and LRR, and comparable to GRPCA. The reason is that SSC needs to compute the spectral decomposition of an  $n \times n$  matrix many times, and both LLR and GRPCA need to compute the SVD of an  $n \times n$  matrix repeatedly. Note that the computational complexities of both spectral decomposition and SVD are as high as  $O(n^3)$ .
- 2) Our model is only slightly slower than SymNMF. Taking the superior clustering performance of our model to SymNMF into consideration, sacrificing a little training time is acceptable.
- 3) The number of samples determines how much time our model will take. How to reduce the computational complexity of our model is left for our future work.

### V. CONCLUSION

In this paper, we have presented a graph-based clustering model that can learn the graph and partition the data simultaneously. Since these two tasks are optimized in a joint manner, the constructed graph is tailored to the task of clustering. Therefore, the clustering performance can be further improved. In addition, the proposed model is numerically solved via an alternating iterative optimization algorithm, where the constraints can be naturally satisfied. The extensive experimental results demonstrate that the proposed model can achieve much better clustering performance than 19 state-of-the-art methods.

The proposed model explores the information from raw features in a linear manner, i.e.,  $\min_{\mathbf{S}} \|\mathbf{X} - \mathbf{X}\mathbf{S}\|_F^2$ . Since Eq. (11) only relates to the inner product of the input (i.e.,  $\mathbf{X}^T\mathbf{X}$ ), the proposed model has potential for exploiting the non-linear relation from the raw features with a kernel trick, which will be investigated in our future work.

### APPENDIX A

#### PROOF OF THEOREM 1

##### A. Proof of *Theorem 1-1*

According to [41], the following **Lemma 1** and **Definition 1** can be used to prove **Theorem 1-1**.

**Definition 1**  $g(h, h')$  is an upper-bound auxiliary function for  $f(h)$  if the following two conditions are satisfied

$$g(h, h') \geq f(h), \text{ and } g(h = h', h') = f(h'). \quad (14)$$

**Lemma 1** If  $g$  is an upper-bound auxiliary function of  $f$ ,  $f$  is decreasing<sup>6</sup> under the update

$$h^* = \underset{h}{\operatorname{argmin}} g(h, h'). \quad (15)$$

See the proof of **Lemma 1** at [41]. Based on **Lemma 1**, if we can find appropriate upper-bound auxiliary functions for Eq. (5) w.r.t.  $\mathbf{S}$  (with the fixed  $\mathbf{V}$ ) and  $\mathbf{V}$  (with the fixed  $\mathbf{S}$ ), respectively, then show the updating rules in Eq. (10) and Eq. (11) decrease the corresponding upper-bound functions, and

<sup>6</sup>non-increasing, to be precise.

together with the fact that Eq. (5) is lower-bounded, **Theorem 1-1** can be proved.

Excluding terms uncorrelated to  $\mathbf{S}$ , the objective function w.r.t.  $\mathbf{S}$  is written as

$$\begin{aligned} \mathcal{O}_{\mathbf{S}} = & \text{Tr} \left( (1 + \beta) \mathbf{S} \mathbf{S}^{\top} + \alpha \mathbf{S} \mathbf{S}^{\top} \mathbf{X}^{\top} \mathbf{X} - 2\alpha \mathbf{X}^{\top} \mathbf{X} \mathbf{S}^{\top} \right. \\ & \left. - 2 \left( \mathbf{V} \mathbf{V}^{\top} + \beta \mathbf{W} \right) \mathbf{S}^{\top} \right) + \text{const.} \\ & \propto \text{Tr} \left( \mathbf{S}^{\top} \mathbf{A} \mathbf{S} - \mathbf{S}^{\top} \mathbf{B} \mathbf{S} - \mathbf{S}^{\top} \mathbf{C} + \mathbf{S}^{\top} \mathbf{D} \right), \end{aligned} \quad (16)$$

where  $\mathbf{A} = (1 + \beta) \mathbf{I} + \alpha (\mathbf{X}^{\top} \mathbf{X})^+$ ,  $\mathbf{B} = \alpha (\mathbf{X}^{\top} \mathbf{X})^-$ ,  $\mathbf{C} = 2\mathbf{V} \mathbf{V}^{\top} + 2\beta \mathbf{W} + 2\alpha (\mathbf{X}^{\top} \mathbf{X})^+$ , and  $\mathbf{D} = 2\mathbf{B} = 2\alpha (\mathbf{X}^{\top} \mathbf{X})^-$ .

For the  $\mathbf{V}$ -block, the corresponding objective function is

$$\begin{aligned} \mathcal{O}_{\mathbf{V}} = & \text{Tr} \left( -2\mathbf{V} \mathbf{V}^{\top} \mathbf{S}^{\top} + \mathbf{V} \mathbf{V}^{\top} \mathbf{V} \mathbf{V}^{\top} \right) + \text{const} \\ & \propto \text{Tr} \left( -2\mathbf{V} \mathbf{V}^{\top} \mathbf{S}^{\top} + \mathbf{V} \mathbf{V}^{\top} \mathbf{V} \mathbf{V}^{\top} \right). \end{aligned} \quad (17)$$

The adopted upper-bound auxiliary functions for Eqs. (16) and (17) are given in the following two lemmas.

**Lemma 2** *The upper bound auxiliary function for Eq. (16) is*

$$\begin{aligned} f_s(\mathbf{S}, \mathbf{S}') = & - \sum_{ijk} \mathbf{B}_{ik} \mathbf{S}'_{kj} \mathbf{S}'_{ij} \left( 1 + \log \frac{\mathbf{S}_{kj} \mathbf{S}_{ij}}{\mathbf{S}'_{kj} \mathbf{S}'_{ij}} \right) \\ & + \sum_{ij} \frac{(\mathbf{A} \mathbf{S}')_{ij} \mathbf{S}_{ij}^2}{\mathbf{S}'_{ij}} + \sum_{ij} \mathbf{D}_{ij} \frac{\mathbf{S}_{ij}^2 + \mathbf{S}'_{ij}{}^2}{2\mathbf{S}'_{ij}} \\ & - \sum_{ij} \mathbf{C}_{ij} \mathbf{S}'_{ij} \left( 1 + \log \frac{\mathbf{S}_{ij}}{\mathbf{S}'_{ij}} \right). \end{aligned} \quad (18)$$

**Lemma 3** *The upper-bound auxiliary function for Eq. (17) is*

$$\begin{aligned} f_v(\mathbf{V}, \mathbf{V}') = & \sum_{ij} \sum_{k=1}^c (\mathbf{V}' \mathbf{V}'^{\top})_{ij} \mathbf{V}'_{ik} \times \frac{\mathbf{V}_{jk}^4}{\mathbf{V}'_{jk}{}^3} \\ & - 2 \sum_{ij} \sum_{k=1}^c \mathbf{S}_{ji} \mathbf{V}'_{jk} \mathbf{V}'_{ik} \left( 1 + \log \frac{\mathbf{V}_{jk} \mathbf{V}_{ik}}{\mathbf{V}'_{jk} \mathbf{V}'_{ik}} \right). \end{aligned} \quad (19)$$

**Proof of Lemma 2:** Lemma 2 can be proved based on the following 4 inequalities.

**Proposition 1** *For any positive matrices  $\mathbf{A} > 0$ ,  $\mathbf{B} > 0$ ,  $\mathbf{C} > 0$ ,  $\mathbf{D} > 0$ ,  $\mathbf{S} > 0$  and  $\mathbf{S}' > 0$ , with  $\mathbf{A}$  symmetric, the following equations hold:*

$$\text{tr}(\mathbf{S}^{\top} \mathbf{A} \mathbf{S}) \leq \sum_{ij} \frac{(\mathbf{A} \mathbf{S}')_{ij} \mathbf{S}_{ij}^2}{\mathbf{S}'_{ij}}, \quad (20a)$$

$$\text{tr}(\mathbf{S}^{\top} \mathbf{B} \mathbf{S}) \geq \sum_{ijk} \mathbf{B}_{jk} \mathbf{S}'_{ki} \mathbf{S}'_{ji} \left( 1 + \log \frac{\mathbf{S}_{ki} \mathbf{S}_{ji}}{\mathbf{S}'_{ki} \mathbf{S}'_{ji}} \right), \quad (20b)$$

$$\text{tr}(\mathbf{S}^{\top} \mathbf{C}) \geq \sum_{ij} \mathbf{C}_{ij} \mathbf{S}'_{ij} \left( 1 + \log \frac{\mathbf{S}_{ij}}{\mathbf{S}'_{ij}} \right), \quad (20c)$$

$$\text{tr}(\mathbf{S}^{\top} \mathbf{D}) \leq \sum_{ij} \mathbf{D}_{ij} \frac{\mathbf{S}_{ij}^2 + \mathbf{S}'_{ij}{}^2}{2\mathbf{S}'_{ij}}. \quad (20d)$$

Moreover, all the equalities hold when  $\mathbf{S} = \mathbf{S}'$ .

See the proofs of those inequalities in Appendix B. According to **Proposition 1**, **Lemma 2** can be easily proved. To find the minimum of Eq. (18), we take

$$\begin{aligned} \frac{\partial f_s(\mathbf{S}_{ij}, \mathbf{S}'_{ij})}{\partial \mathbf{S}_{ij}} = & \frac{2(\mathbf{A} \mathbf{S}')_{ij} \mathbf{S}_{ij}}{\mathbf{S}'_{ij}} - \frac{(\mathbf{B} \mathbf{S}')_{ij} \mathbf{S}'_{ij}}{\mathbf{S}_{ij}} \\ & - \frac{(\mathbf{B}^{\top} \mathbf{S}')_{ij} \mathbf{S}'_{ij}}{\mathbf{S}_{ij}} + \mathbf{D}_{ij} \frac{\mathbf{S}_{ij}}{\mathbf{S}'_{ij}} - \mathbf{C}_{ij} \frac{\mathbf{S}'_{ij}}{\mathbf{S}_{ij}}. \end{aligned} \quad (21)$$

The detailed calculation of those derivatives can be found in Appendix C. Moreover, the Hessian matrix containing the second order derivatives

$$\begin{aligned} \frac{\partial^2 f_s(\mathbf{S}, \mathbf{S}')}{\mathbf{S}_{ij} \mathbf{S}_{lk}} = & \delta_{il} \delta_{jk} \frac{2(\mathbf{A} \mathbf{S}')_{ij} + \mathbf{D}_{ij}}{\mathbf{S}'_{ij}} \\ & + \delta_{il} \delta_{jk} \frac{2(\mathbf{B} \mathbf{S}')_{ij} \mathbf{S}'_{ij} + \mathbf{C}_{ij} \mathbf{S}'_{ij}}{\mathbf{S}_{ij}^2} \end{aligned} \quad (22)$$

is a diagonal matrix with each element no less than 0, where  $\delta_{ij}$  is a delta function, i.e.,

$$\delta_{ij} = \begin{cases} 1, & \text{if } i = j, \\ 0, & \text{if } i \neq j. \end{cases} \quad (23)$$

Therefore, Eq. (18) is a convex function, where we can get its global minimization by setting  $\frac{\partial f_s(\mathbf{S}, \mathbf{S}')}{\partial \mathbf{S}_{ij}} = 0$ , i.e.,

$$\begin{aligned} \mathbf{S}_{ij} = & \mathbf{S}'_{ij} \sqrt{\frac{\mathbf{C}_{ij} + 2(\mathbf{B} \mathbf{S}')_{ij}}{2(\mathbf{A} \mathbf{S}')_{ij} + \mathbf{D}_{ij}}} = \\ & \mathbf{S}'_{ij} \sqrt{\frac{(\mathbf{V} \mathbf{V}^{\top} + \beta \mathbf{W} + \alpha (\mathbf{X}^{\top} \mathbf{X})^+ + \alpha (\mathbf{X}^{\top} \mathbf{X})^- \mathbf{S}')_{ij}}{(\mathbf{S}' + \beta \mathbf{S}' + \alpha (\mathbf{X}^{\top} \mathbf{X})^+ \mathbf{S}' + \alpha (\mathbf{X}^{\top} \mathbf{X})^-)_{ij}}}, \end{aligned} \quad (24)$$

which is exactly the same as Eq. (10). Accordingly, we can conclude that the S-step decreases the objective function of Eq. (5) according to **Lemma 1**.

**Proof of Lemma 3:** Lemma 3 can be proved based on the following 2 inequalities.

**Proposition 2** *For any positive matrices  $\mathbf{V} > 0$ ,  $\mathbf{S} > 0$  and  $\mathbf{V}' > 0$ , the following equations hold:*

$$\text{Tr}(\mathbf{V} \mathbf{V}^{\top} \mathbf{V} \mathbf{V}^{\top}) \leq \sum_{ij} \sum_{k=1}^c (\mathbf{V}' \mathbf{V}'^{\top})_{ij} \mathbf{V}'_{ik} \times \frac{\mathbf{V}_{jk}^4}{\mathbf{V}'_{jk}{}^3}, \quad (25a)$$

$$\text{Tr}(-\mathbf{S} \mathbf{V} \mathbf{V}^{\top}) \leq - \sum_{ij} \sum_{k=1}^c \mathbf{S}_{ji} \mathbf{V}'_{jk} \mathbf{V}'_{ik} \left( 1 + \log \frac{\mathbf{V}_{ik} \mathbf{V}_{jk}}{\mathbf{V}'_{ik} \mathbf{V}'_{jk}} \right). \quad (25b)$$

Moreover, all the equalities hold when  $\mathbf{V} = \mathbf{V}'$ .

See the proof of **Proposition 2** in Appendix B. Let's take

$$\begin{aligned} \frac{\partial f_v(\mathbf{V}, \mathbf{V}')}{\partial \mathbf{V}_{jk}} = & -2 \frac{(\mathbf{S} \mathbf{V}')_{jk} \mathbf{V}'_{jk}}{\mathbf{V}_{jk}} - 2 \frac{(\mathbf{S}^{\top} \mathbf{V}')_{jk} \mathbf{V}'_{jk}}{\mathbf{V}_{jk}} \\ & + 4 \left( \mathbf{V}' \mathbf{V}'^{\top} \mathbf{V}' \right)_{jk} \frac{\mathbf{V}_{jk}^3}{\mathbf{V}'_{jk}{}^3}. \end{aligned} \quad (26)$$

$f_v(\mathbf{V}, \mathbf{V}')$ 's Hessian matrix is also a positive diagonal matrix with

$$\begin{aligned} \frac{\partial^2 f_v(\mathbf{V}, \mathbf{V}')}{\partial \mathbf{V}_{jk} \partial \mathbf{V}_{il}} &= 12\delta_{ji}\delta_{kl} \left( \mathbf{V}' \mathbf{V}'^T \mathbf{V}' \right)_{jk} \frac{\mathbf{V}'_{jk}}{\mathbf{V}'_{jk}{}^3} \\ &+ 2\delta_{ji}\delta_{kl} \frac{(\mathbf{S}\mathbf{V}')_{jk} \mathbf{V}'_{jk}}{\mathbf{V}'_{jk}{}^2} + 2\delta_{ji}\delta_{kl} \frac{(\mathbf{S}^T \mathbf{V}')_{jk} \mathbf{V}'_{jk}}{\mathbf{V}'_{jk}{}^2}. \end{aligned} \quad (27)$$

Therefore,  $f_v(\mathbf{V}, \mathbf{V}')$  is convex w.r.t.  $\mathbf{V}_{jk}$ . Let  $\frac{\partial g(\mathbf{V}, \mathbf{V}')}{\partial \mathbf{V}_{jk}} = 0$ , we get the minimum of  $f_v(\mathbf{V}, \mathbf{V}')$  at

$$\mathbf{V}_{jk} = \mathbf{V}'_{jk} \times \sqrt[4]{\frac{(\mathbf{S}\mathbf{V}')_{jk} + (\mathbf{S}^T \mathbf{V}')_{jk}}{2(\mathbf{V}' \mathbf{V}'^T \mathbf{V}')_{jk}}} \quad (28)$$

which is exactly the same as Eq. (11). Accordingly, we can conclude that the V-step decreases the objective function of Eq. (5). In addition, it is apparent that Eq. (5) is lower-bounded by 0. The proof of **Theorem 1-1** is complete.

### B. Proof of Theorem 1-2

At the first iteration, for  $i \neq j$ , we have

$$\begin{aligned} \mathbf{S}_{ij}^1 &= \\ \mathbf{S}_{ij}^0 &\left( \frac{\left( \mathbf{V}^0 \mathbf{V}^{0T} + \alpha (\mathbf{X}^T \mathbf{X})^+ + \alpha (\mathbf{X}^T \mathbf{X})^- \mathbf{S}^0 + \beta \mathbf{W} \right)_{ij}}{\left( \mathbf{S}^0 + \alpha (\mathbf{X}^T \mathbf{X})^+ \mathbf{S}^0 + \alpha (\mathbf{X}^T \mathbf{X})^- + \beta \mathbf{S}^0 \right)_{ij}} \right)^{\frac{1}{2}}. \end{aligned} \quad (29)$$

Since

$$\begin{aligned} &\left( \mathbf{V}^0 \mathbf{V}^{0T} + \alpha (\mathbf{X}^T \mathbf{X})^+ + \alpha (\mathbf{X}^T \mathbf{X})^- \mathbf{S}^0 + \beta \mathbf{W} \right)_{ij} \\ &\geq \left( \mathbf{V}^0 \mathbf{V}^{0T} \right)_{ij} > 0, \end{aligned} \quad (30)$$

and

$$\left( \mathbf{S}^0 + \alpha (\mathbf{X}^T \mathbf{X})^+ \mathbf{S}^0 + \alpha (\mathbf{X}^T \mathbf{X})^- + \beta \mathbf{S}^0 \right)_{ij} \geq \mathbf{S}_{ij}^0 > 0, \quad (31)$$

we have  $\mathbf{S}_{ij}^1 > 0, \forall i, j$ , and,  $i \neq j$ .

For  $\mathbf{S}_{ii}^1, \forall i$ , we have

$$\begin{aligned} \mathbf{S}_{ii}^1 &= \mathbf{S}_{ii}^0 \left( \frac{\left( \mathbf{V}^0 \mathbf{V}^{0T} + \alpha (\mathbf{X}^T \mathbf{X})^+ + \alpha (\mathbf{X}^T \mathbf{X})^- \mathbf{S}^0 + \beta \mathbf{W} \right)_{ii}}{\left( \mathbf{S}^0 + \alpha (\mathbf{X}^T \mathbf{X})^+ \mathbf{S}^0 + \alpha (\mathbf{X}^T \mathbf{X})^- + \beta \mathbf{S}^0 \right)_{ii}} \right)^{\frac{1}{2}} \\ &= 0 \times \left( \frac{\left( \mathbf{V}^0 \mathbf{V}^{0T} + \alpha (\mathbf{X}^T \mathbf{X})^+ + \alpha (\mathbf{X}^T \mathbf{X})^- \mathbf{S}^0 + \beta \mathbf{W} \right)_{ii}}{\left( \mathbf{S}^0 + \alpha (\mathbf{X}^T \mathbf{X})^+ \mathbf{S}^0 + \alpha (\mathbf{X}^T \mathbf{X})^- + \beta \mathbf{S}^0 \right)_{ii}} \right)^{\frac{1}{2}} \\ &= 0. \end{aligned} \quad (32)$$

To avoid the possible numerical inaccuracy caused by the extreme small values in the denominator of Eq. (32), we could add a small positive value in the denominator. Note that, this additional process does not change the value of  $\mathbf{S}_{ii}^1, \forall i$ .

For  $\mathbf{V}_{ij}^1, \forall i, j$ , we have

$$\mathbf{V}_{ij}^1 = \mathbf{V}_{ij}^0 \left( \frac{\left( \mathbf{S}^1 \mathbf{V}^0 + \mathbf{S}^{1T} \mathbf{V}^0 \right)_{ij}}{\left( 2\mathbf{V}^0 \mathbf{V}^{0T} \mathbf{V}^0 \right)_{ij}} \right)^{\frac{1}{4}}. \quad (33)$$

Since  $\left( \mathbf{S}^1 \mathbf{V}^0 + \mathbf{S}^{1T} \mathbf{V}^0 \right)_{ij} = \sum_k \left( \mathbf{S}_{ik}^1 \mathbf{V}_{kj}^0 + \mathbf{S}_{ik}^{1T} \mathbf{V}_{kj}^0 \right) \geq \sum_{k \neq i} \mathbf{S}_{ik}^1 \mathbf{V}_{kj}^0 > 0$ , and  $\left( 2\mathbf{V}^0 \mathbf{V}^{0T} \mathbf{V}^0 \right)_{ij} > 0$ , we have  $\mathbf{V}_{ij}^1 > 0, \forall i, j$ .

Based on the above analysis, we get that

$$\mathbf{V}_{ij}^1 > 0, \forall i, j, \text{ and } \begin{cases} \mathbf{S}_{ij}^1 > 0, \forall i, j, \text{ and } i \neq j \\ \mathbf{S}_{ii}^1 = 0, \forall i. \end{cases} \quad (34)$$

According to mathematical induction, the **Theorem 1-2** can be proved. Another additional advantage of our algorithm is that at each iteration  $\text{diag}(\mathbf{S}^t) = 0$  holds, such that our algorithm can remove the trivial solution naturally.

## APPENDIX B

### PROOF OF PROPOSITIONS 1 AND 2

#### A. Proof of Proposition 1

**Proof of Eq. (20a):** Let  $\mathbf{S}_{ij} = u_{ij} \mathbf{S}'_{ij}$  and  $u_{ij} > 0, \forall ij$ , we have

$$\begin{aligned} &\sum_{ij} \frac{(\mathbf{A}\mathbf{S}')_{ij} \mathbf{S}_{ij}^2}{\mathbf{S}'_{ij}} - \text{tr}(\mathbf{S}^T \mathbf{A}\mathbf{S}) \\ &= \sum_{ijk} \mathbf{A}_{ik} \mathbf{S}'_{kj} \mathbf{S}'_{ij} u_{ij}^2 - \sum_{ijk} \mathbf{A}_{ik} \mathbf{S}'_{kj} \mathbf{S}'_{ij} u_{ij} u_{kj} = \Delta \end{aligned} \quad (35)$$

Since  $\mathbf{A}$  is a symmetric matrix, we can exchange the indicator ( $ik$ ) in Eq. (35) and get

$$\Delta = \sum_{ijk} \mathbf{A}_{ik} \mathbf{S}'_{kj} \mathbf{S}'_{ij} u_{kj}^2 - \sum_{ijk} \mathbf{A}_{ik} \mathbf{S}'_{kj} \mathbf{S}'_{ij} u_{ij} u_{kj}. \quad (36)$$

Combining Eq. (35) and Eq. (36) together, we have

$$\Delta = \frac{1}{2} \sum_{ijk} \mathbf{A}_{ik} \mathbf{S}'_{kj} \mathbf{S}'_{ij} (u_{kj}^2 + u_{ij}^2 - 2u_{ij} u_{kj}) \geq 0 \quad (37)$$

Thus, Eq. (20a) holds.

**The proof of Eq. (20b):**

$$\begin{aligned} &\text{tr}(\mathbf{S}^T \mathbf{B}\mathbf{S}) - \sum_{ijk} \mathbf{B}_{jk} \mathbf{S}'_{ki} \mathbf{S}'_{ji} \left( 1 + \log \frac{\mathbf{S}_{ki} \mathbf{S}_{ji}}{\mathbf{S}'_{ki} \mathbf{S}'_{ji}} \right) = \\ &\sum_{ijk} \mathbf{B}_{jk} \mathbf{S}_{ki} \mathbf{S}_{ji} - \sum_{ijk} \mathbf{B}_{jk} \mathbf{S}'_{ki} \mathbf{S}'_{ji} \left( 1 + \log \frac{\mathbf{S}_{ki} \mathbf{S}_{ji}}{\mathbf{S}'_{ki} \mathbf{S}'_{ji}} \right). \end{aligned} \quad (38)$$

According to the inequality  $x > 1 + \log(x), \forall x > 0$ , and let  $x = \frac{\mathbf{S}_{ki} \mathbf{S}_{ji}}{\mathbf{S}'_{ki} \mathbf{S}'_{ji}}$ , we can prove Eq. (38)  $\geq 0$  holds and likewise Eq. (20b).

**Proof of Eq. (20c):**

$$\begin{aligned} &\text{tr}(\mathbf{S}^T \mathbf{C}) - \sum_{ij} \mathbf{C}_{ij} \mathbf{S}'_{ij} \left( 1 + \log \frac{\mathbf{S}_{ij}}{\mathbf{S}'_{ij}} \right) \\ &= \sum_{ij} \mathbf{C}_{ij} \mathbf{S}_{ij} - \sum_{ij} \mathbf{C}_{ij} \mathbf{S}'_{ij} \left( 1 + \log \frac{\mathbf{S}_{ij}}{\mathbf{S}'_{ij}} \right). \end{aligned} \quad (39)$$

According to inequality  $x > 1 + \log(x), \forall x > 0$ , and let  $x = \frac{\mathbf{S}_{ij}}{\mathbf{S}'_{ij}}$ , we can prove Eq. (39)  $\geq 0$  holds and likewise Eq. (20c).

**Proof of Eq. (20d):**

$$\begin{aligned} \text{tr}(\mathbf{S}^\top \mathbf{D}) - \sum_{i,j} \mathbf{D}_{ij} \frac{\mathbf{S}_{ij}^2 + \mathbf{S}'_{ij}{}^2}{2\mathbf{S}'_{ij}} \\ = \sum_{ij} \mathbf{S}_{ij} \mathbf{D}_{ij} - \sum_{ij} \mathbf{D}_{ij} \frac{\mathbf{S}_{ij}^2 + \mathbf{S}'_{ij}{}^2}{2\mathbf{S}'_{ij}}. \end{aligned} \quad (40)$$

According to the Janson inequality  $a^2 + b^2 - 2ab \geq 0, \forall a, b$ , and let  $a = \mathbf{S}_{ij}$ ,  $b = \mathbf{S}'_{ij}$ , we can prove Eq. (40)  $\leq 0$  holds and likewise Eq. (20d).

Besides, for all the functions, the equality hold when  $\mathbf{S} = \mathbf{S}'$ , and thus the proof of **Proposition 1** is complete.

### B. Proof of Proposition 2

**Proof of Eq. (25a):** Let  $\mathbf{V}_{ij} = u_{ij} \mathbf{V}'_{ij}$  and  $u_{ij} > 0, \forall i, j$ , and  $u_{ij} > 0$ , we have

$$\begin{aligned} \sum_{ij} \sum_{k=1}^c (\mathbf{V}' \mathbf{V}'^\top)_{ij} \mathbf{V}'_{ik} \times \frac{\mathbf{V}'_{jk}{}^4}{\mathbf{V}'_{jk}} - \text{Tr}(\mathbf{V} \mathbf{V}^\top \mathbf{V} \mathbf{V}^\top) \\ = \sum_{ij} \sum_{kl} \mathbf{V}'_{il} \mathbf{V}'_{jl} \mathbf{V}'_{ik} \mathbf{V}'_{jk} u_{jk}^4 \\ - \sum_{ij} \sum_{kl} \mathbf{V}'_{il} \mathbf{V}'_{jl} \mathbf{V}'_{ik} \mathbf{V}'_{jk} u_{il} u_{jl} u_{ik} u_{jk} = \Delta. \end{aligned} \quad (41)$$

Denote  $\gamma = \sum_{ij} \sum_{kl} \mathbf{V}'_{il} \mathbf{V}'_{jl} \mathbf{V}'_{ik} \mathbf{V}'_{jk} u_{il} u_{jl} u_{ik} u_{jk}$ , exchanging the indicators  $i$  and  $j$  in Eq. (41), we have

$$\Delta = \sum_{ij} \sum_{kl} \mathbf{V}'_{il} \mathbf{V}'_{jl} \mathbf{V}'_{ik} \mathbf{V}'_{jk} u_{ik}^4 - \gamma. \quad (42)$$

Exchanging the indicators  $k$  and  $l$  in Eq. (41), we have

$$\Delta = \sum_{ij} \sum_{kl} \mathbf{V}'_{il} \mathbf{V}'_{jl} \mathbf{V}'_{ik} \mathbf{V}'_{jk} u_{jl}^4 - \gamma. \quad (43)$$

Exchanging the indicators  $ik$  and  $jl$  in Eq. (41), we have

$$\Delta = \sum_{ij} \sum_{kl} \mathbf{V}'_{il} \mathbf{V}'_{jl} \mathbf{V}'_{ik} \mathbf{V}'_{jk} u_{il}^4 - \gamma. \quad (44)$$

Combining Eqs (41)-(44) together, we have

$$\begin{aligned} \Delta = \sum_{ij} \sum_{kl} \mathbf{V}'_{il} \mathbf{V}'_{jl} \mathbf{V}'_{ik} \mathbf{V}'_{jk} \left( \frac{u_{il}^4 + u_{jl}^4 + u_{ik}^4 + u_{jk}^4}{4} \right. \\ \left. - u_{il} u_{jl} u_{ik} u_{jk} \right) \geq \sum_{ij} \sum_{kl} \mathbf{V}'_{il} \mathbf{V}'_{jl} \mathbf{V}'_{ik} \mathbf{V}'_{jk} \times \\ \left( \frac{u_{il}^2 u_{jl}^2 + u_{ik}^2 u_{jk}^2}{2} - u_{il} u_{jl} u_{ik} u_{jk} \right) \geq 0. \end{aligned} \quad (45)$$

Together with the fact that the equality holds when  $\mathbf{V} = \mathbf{V}'$ , the proof of Eq. (25a) is completed.

**Proof of Eq. (25b):** The proof of Eq. (25b) is equivalent to the proof of Eq. (20b).

### APPENDIX C DERIVATE OF EQ. (20)

Here, we only present how to calculate the derivate of Eq. (20)-b, as those of Eq. (20)-a, Eq. (20)-c and Eq. (20)-d are easy to solve.

Let  $f = \sum_{ijk} \mathbf{B}_{jk} \mathbf{S}'_{ki} \mathbf{S}'_{ji} \left( 1 + \log \frac{\mathbf{S}_{ki} \mathbf{S}_{ji}}{\mathbf{S}'_{ki} \mathbf{S}'_{ji}} \right) \propto \sum_{ijk} \mathbf{B}_{jk} \mathbf{S}'_{ki} \mathbf{S}'_{ji} (\log \mathbf{S}_{ki} + \log \mathbf{S}_{ji})$ , to calculate the derivative of  $f$  with respect to  $\mathbf{S}_{ij}$ , we separate  $f = f_1 + f_2$ , where  $f_1 = \sum_{ijk} \mathbf{B}_{jk} \mathbf{S}'_{ki} \mathbf{S}'_{ji} (\log \mathbf{S}_{ki})$  and  $f_2 = \sum_{ijk} \mathbf{B}_{jk} \mathbf{S}'_{ki} \mathbf{S}'_{ji} (\log \mathbf{S}_{ji})$ . Particularly, exchanging  $i$  with  $j$  in  $f_1$ , we have  $f_1 = \sum_{ijk} \mathbf{B}_{ik} \mathbf{S}'_{kj} \mathbf{S}'_{ij} (\log \mathbf{S}_{kj})$ . Then exchanging  $i$  and  $k$ , we have  $f_1 = \sum_{ijk} \mathbf{B}_{ki} \mathbf{S}'_{ij} \mathbf{S}'_{kj} (\log \mathbf{S}_{ij})$ . Accordingly,

$$\frac{\partial f_1}{\partial \mathbf{S}_{ij}} = \frac{\sum_k \mathbf{B}_{ki} \mathbf{S}'_{kj} \mathbf{S}'_{ij}}{\mathbf{S}_{ij}} = \frac{(\mathbf{B}^\top \mathbf{S}')_{ij} \mathbf{S}'_{ij}}{\mathbf{S}_{ij}}. \quad (46)$$

Exchanging  $i$  with  $j$  in  $f_2$ , we have  $f_2 = \sum_{ijk} \mathbf{B}_{ik} \mathbf{S}'_{kj} \mathbf{S}'_{ij} (\log \mathbf{S}_{ij})$ . Accordingly,

$$\frac{\partial f_2}{\partial \mathbf{S}_{ij}} = \frac{\sum_k \mathbf{B}_{ik} \mathbf{S}'_{kj} \mathbf{S}'_{ij}}{\mathbf{S}_{ij}} = \frac{(\mathbf{B} \mathbf{S}')_{ij} \mathbf{S}'_{ij}}{\mathbf{S}_{ij}}. \quad (47)$$

Finally, the corresponding derivative is

$$\frac{\partial f}{\partial \mathbf{S}_{ij}} = \frac{(\mathbf{B} \mathbf{S}')_{ij} \mathbf{S}'_{ij}}{\mathbf{S}_{ij}} + \frac{(\mathbf{B}^\top \mathbf{S}')_{ij} \mathbf{S}'_{ij}}{\mathbf{S}_{ij}}. \quad (48)$$

When  $\mathbf{B}$  is a symmetric matrix, we have

$$\frac{\partial f}{\partial \mathbf{S}_{ij}} = \frac{2(\mathbf{B} \mathbf{S}')_{ij} \mathbf{S}'_{ij}}{\mathbf{S}_{ij}}. \quad (49)$$

### REFERENCES

- [1] Z. Wu and R. Leahy, "An optimal graph theoretic approach to data clustering: Theory and its application to image segmentation," *IEEE Trans. Pattern Anal. Mach. Intell.*, vol. 15, no. 11, pp. 1101–1113, 1993.
- [2] K.-S. Chuang, H.-L. Tzeng, S. Chen, J. Wu, and T.-J. Chen, "Fuzzy c-means clustering with spatial information for image segmentation," *Computerized Medical Imaging and Graphics*, vol. 30, no. 1, pp. 9–15, 2006.
- [3] W. Wu, Y. Jia, S. Kwong, and J. Hou, "Pairwise constraint propagation-induced symmetric nonnegative matrix factorization," *IEEE Trans. Neural Netw. Learn. Syst.*, vol. 29, no. 12, pp. 6348–6361, Dec 2018.
- [4] W. Wu, S. Kwong, Y. Zhou, Y. Jia, and W. Gao, "Nonnegative matrix factorization with mixed hypergraph regularization for community detection," *Information Sciences*, vol. 435, pp. 263–281, 2018.
- [5] J. Das, P. Mukherjee, S. Majumder, and P. Gupta, "Clustering-based recommender system using principles of voting theory," in *Proc. IC3I*. IEEE, 2014, pp. 230–235.
- [6] Z. Yu, H. Chen, J. You, H.-S. Wong, J. Liu, L. Li, and G. Han, "Double selection based semi-supervised clustering ensemble for tumor clustering from gene expression profiles," *IEEE/ACM Trans. Comput. Biol. Bioinf.*, vol. 11, no. 4, pp. 727–740, 2014.
- [7] Z. Yu, L. Li, J. You, H.-S. Wong, and G. Han, "Sc<sup>3</sup>: Triple spectral clustering-based consensus clustering framework for class discovery from cancer gene expression profiles," *IEEE/ACM Trans. Comput. Biol. Bioinf.*, vol. 9, no. 6, pp. 1751–1765, 2012.
- [8] Z. Yu, H.-S. Wong, and H. Wang, "Graph-based consensus clustering for class discovery from gene expression data," *Bioinformatics*, vol. 23, no. 21, pp. 2888–2896, 2007.
- [9] A. N. Gorban, B. Kégl, D. C. Wunsch, A. Y. Zinovyev *et al.*, *Principal manifolds for data visualization and dimension reduction*. Springer, 2008, vol. 58.

- [10] B. Jian and B. C. Vemuri, "Robust point set registration using gaussian mixture models," *IEEE Trans. Pattern Anal. Mach. Intell.*, vol. 33, no. 8, pp. 1633–1645, 2011.
- [11] D. Comaniciu and P. Meer, "Mean shift: A robust approach toward feature space analysis," *IEEE Trans. Pattern Anal. Mach. Intell.*, no. 5, pp. 603–619, 2002.
- [12] Y. Cheng, "Mean shift, mode seeking, and clustering," *IEEE Trans. Pattern Anal. Mach. Intell.*, vol. 17, no. 8, pp. 790–799, 1995.
- [13] A. Y. Ng, M. I. Jordan, and Y. Weiss, "On spectral clustering: Analysis and an algorithm," in *Proc. AAAI*, 2002, pp. 849–856.
- [14] Y. Yang, H. T. Shen, F. Nie, R. Ji, and X. Zhou, "Nonnegative spectral clustering with discriminative regularization," in *Proc. AAAI*, 2011.
- [15] D. Kuang, S. Yun, and H. Park, "Symmmf: nonnegative low-rank approximation of a similarity matrix for graph clustering," *Journal of Global Optimization*, vol. 62, no. 3, pp. 545–574, 2015.
- [16] D. Kuang, C. Ding, and H. Park, "Symmetric nonnegative matrix factorization for graph clustering," in *Proc. ICDM*. SIAM, 2012, pp. 106–117.
- [17] L. Zelnik-Manor and P. Perona, "Self-tuning spectral clustering," in *Proc. NIPS*, 2005, pp. 1601–1608.
- [18] B. Cheng, J. Yang, S. Yan, Y. Fu, and T. S. Huang, "Learning with  $\ell^1$ -graph for image analysis," *IEEE Trans. Image Process.*, vol. 19, no. 4, pp. 858–866, April 2010.
- [19] G. Liu, Z. Lin, and Y. Yu, "Robust subspace segmentation by low-rank representation," in *Proc. ICML*, 2010, pp. 663–670.
- [20] E. Elhamifar and R. Vidal, "Sparse subspace clustering," in *Proc. CVPR*. IEEE, 2009, pp. 2790–2797.
- [21] X. Peng, Z. Yu, Z. Yi, and H. Tang, "Constructing the  $l_2$ -graph for robust subspace learning and subspace clustering," *IEEE Trans. Cybern.*, vol. 47, no. 4, pp. 1053–1066, 2017.
- [22] F. Nie, X. Wang, and H. Huang, "Clustering and projected clustering with adaptive neighbors," in *Proc. SIGKDD*. ACM, 2014, pp. 977–986.
- [23] X. Dong, D. Thanou, P. Frossard, and P. Vandergheynst, "Learning laplacian matrix in smooth graph signal representations," *IEEE Trans. Signal Process.*, vol. 64, no. 23, pp. 6160–6173, 2016.
- [24] C.-G. Li, C. You, and R. Vidal, "Structured sparse subspace clustering: A joint affinity learning and subspace clustering framework," *IEEE Trans. Image Process.*, vol. 26, no. 6, pp. 2988–3001, 2017.
- [25] C.-G. Li, Z. Lin, H. Zhang, and J. Guo, "Learning semi-supervised representation towards a unified optimization framework for semi-supervised learning," in *Proc. ICCV*, 2015, pp. 2767–2775.
- [26] X. Fang, Y. Xu, X. Li, Z. Lai, and W. K. Wong, "Robust semi-supervised subspace clustering via non-negative low-rank representation," *IEEE Trans. Cybern.*, vol. 46, no. 8, pp. 1828–1838, 2016.
- [27] Z. Lai, D. Mo, J. Wen, L. Shen, and W. Wong, "Generalized robust regression for jointly sparse subspace learning," *IEEE Trans. Circuits Syst. Video Technol.*, 2018.
- [28] Z. Zhang, Y. Zhang, G. Liu, J. Tang, S. Yan, and M. Wang, "Joint label prediction based semi-supervised adaptive concept factorization for robust data representation," *IEEE Trans. Knowl. Data Eng.*, 2019.
- [29] F. Nie, S. J. Shi, and X. Li, "Semi-supervised learning with auto-weighting feature and adaptive graph," *IEEE Trans. Knowl. Data Eng.*, 2019.
- [30] U. Von Luxburg, "A tutorial on spectral clustering," *Statistics and Computing*, vol. 17, no. 4, pp. 395–416, 2007.
- [31] X. Dong, D. Thanou, M. Rabbat, and P. Frossard, "Learning graphs from data: A signal representation perspective," *IEEE Signal Process. Mag.*, vol. 36, no. 3, pp. 44–63, 2019.
- [32] E. Pavez and A. Ortega, "Generalized laplacian precision matrix estimation for graph signal processing," in *Proc. ICASSP*. IEEE, 2016, pp. 6350–6354.
- [33] V. Kalofolias, "How to learn a graph from smooth signals," in *Artificial Intelligence and Statistics*, 2016, pp. 920–929.
- [34] S. P. Chepuri, S. Liu, G. Leus, and A. O. Hero, "Learning sparse graphs under smoothness prior," in *Proc. ICASSP*. IEEE, 2017, pp. 6508–6512.
- [35] C. Lu, S. Yan, and Z. Lin, "Convex sparse spectral clustering: Single-view to multi-view," *IEEE Trans. Image Process.*, vol. 25, no. 6, pp. 2833–2843, 2016.
- [36] C.-Y. Lu, H. Min, Z.-Q. Zhao, L. Zhu, D.-S. Huang, and S. Yan, "Robust and efficient subspace segmentation via least squares regression," in *Proc. ECCV*. Springer, 2012, pp. 347–360.
- [37] Y. Jia, S. Kwong, W. Wu, R. Wang, and W. Gao, "Sparse bayesian learning-based kernel poisson regression," *IEEE Trans. Cybern.*, vol. 49, no. 1, p. 56, 2019.
- [38] J. Wright, A. Ganesh, S. Rao, Y. Peng, and Y. Ma, "Robust principal component analysis: Exact recovery of corrupted low-rank matrices via convex optimization," in *Proc. NIPS*, 2009, pp. 2080–2088.
- [39] E. J. Candès, X. Li, Y. Ma, and J. Wright, "Robust principal component analysis?" *Journal of the ACM*, vol. 58, no. 3, p. 11, 2011.
- [40] B. Jiang, C. Ding, B. Luo, and J. Tang, "Graph-laplacian pca: Closed-form solution and robustness," in *Proc. CVPR*, 2013, pp. 3492–3498.
- [41] D. D. Lee and H. S. Seung, "Algorithms for non-negative matrix factorization," in *Proc. NIPS*, 2001, pp. 556–562.
- [42] D. Cai, X. He, J. Han, and T. S. Huang, "Graph regularized nonnegative matrix factorization for data representation," *IEEE Trans. Pattern Anal. Mach. Intell.*, vol. 33, no. 8, pp. 1548–1560, 2011.
- [43] Z. Zhang and K. Zhao, "Low-rank matrix approximation with manifold regularization," *IEEE Trans. Pattern Anal. Mach. Intell.*, vol. 35, no. 7, pp. 1717–1729, 2013.
- [44] N. Shahid, V. Kalofolias, X. Bresson, M. Bronstein, and P. Vandergheynst, "Robust principal component analysis on graphs," in *Proc. CVPR*, 2015, pp. 2812–2820.
- [45] G. Liu, Z. Lin, S. Yan, J. Sun, Y. Yu, and Y. Ma, "Robust recovery of subspace structures by low-rank representation," *IEEE Trans. Pattern Anal. Mach. Intell.*, vol. 35, no. 1, pp. 171–184, 2013.
- [46] X. Guo, "Robust subspace segmentation by simultaneously learning data representations and their affinity matrix," in *Proc. IJCAI*. AAAI Press, 2015, pp. 3547–3553.
- [47] H. E. Egilmez, E. Pavez, and A. Ortega, "Graph learning from data under laplacian and structural constraints," *IEEE J. Sel. Topics Signal Process.*, vol. 11, no. 6, pp. 825–841, 2017.
- [48] D. Cai, X. He, and J. Han, "Document clustering using locality preserving indexing," *IEEE Trans. Knowl. Data Eng.*, vol. 17, no. 12, pp. 1624–1637, 2005.
- [49] C. Ding, X. He, and H. D. Simon, "On the equivalence of nonnegative matrix factorization and spectral clustering," in *Proc. ICDM*. SIAM, 2005, pp. 606–610.
- [50] C. Ding and X. He, "K-means clustering via principal component analysis," in *Proc. ICML*. ACM, 2004, p. 29.
- [51] D. Kong, C. Ding, H. Huang, and F. Nie, "An iterative locally linear embedding algorithm," in *Proc. ICML*. Omnipress, 2012, pp. 931–938.
- [52] V. Y. Tan and C. Févotte, "Automatic relevance determination in nonnegative matrix factorization with the/spl beta/-divergence," *IEEE Trans. Pattern Anal. Mach. Intell.*, vol. 35, no. 7, pp. 1592–1605, 2012.